CME LIVE OPEN ACCESS

Journal of
Earth & Environmental Waste Management

Research Article

Spatial Analysis of Water Budget Components in the Upper Awash River Sub-basin, Ethiopia Using SWAT Model

A. Muauz[1*], B. Berehanu[2] and H. Bedru[3]

[1]Ethiopian Institute of Water Resource, Addis Ababa University, Addis Ababa, Ethiopia.*

[2]School of Erath Sciences, Addis Ababa University, Addis Ababa, Ethiopia.

[3]School of Erath Sciences and Engineering, Addis Ababa Science and Technology University, Addis Ababa, Ethiopia.

Corresponding Author: A. Muauz, Ethiopian Institute of Water Resource, Addis Ababa University, Addis Ababa, Ethiopia.

Received: 2024 Jun 05 **Accepted:** 2024 Jun 25 **Published:** 2024 Jul 04

Abstract

The study used the SWAT model to analyze water budget components in the Upper Awash River sub-basin. Data spanning 1986 to 2013 underwent calibration from 1988 to 2008, preceded by a three-year warm-up period, followed by validation over five years at two gauging stations. Sensitivity analyses utilized t-stat and p-value, while model uncertainty was assessed using p-factor and r-factor indices. Model performance was evaluated with NSE, R2, and PBIAS. Calibration and validation produced p-factors and r-factors of 0.801, 0.9 for Hombele, and 0.808, 0.98 for Melkakuntro. R2, NSE, and PBIAS values during calibration were 0.82, 0.82, -2.3 for Hombele, and 0.79, 0.78, -13.1 for Melkakuntro. Validation values were 0.71, 0.67, 11.2 for Hombele, and 0.7, 0.66, 1.9 for Melkakuntro. The average annual groundwater recharge rate varied from 0 to 904.3 mm, totaling 181.1 mm/yr constituting about 19.1% of mean annual precipitation. The simulated mean annual surface runoff and evapotranspiration in the Upper Awash sub-basin were 93.4 and 682.5 mm, respectively. These accounted for 9.8% and 71.8% of the mean annual precipitation, respectively. These findings offer valuable insights into the water system of the Upper Awash River sub-basin, enhancing our understanding of its complexity. This information can support sustainable water management practices in the area.

Keywords: Model Uncertainty Analysis, Performance Evaluation, Sensitivity Analysis, Upper Awash Sub-Basin, Water Budget Components, SWAT Model.

1. Introduction

The sustainable utilization of water resources has become increasingly challenging due to the uneven distribution of available water resources and the alarming increase in water demand. This demand is driven by factors such as population growth, urbanization, industrialization, and agricultural expansions [1, 2].

The Awash River Basin is currently experiencing a significant increase in water demand due to rapid population growth and ongoing socioeconomic development in the area. This surge in demand has led to increased rivalry among various water users within the sub-basins of the Awash River Basin, placing immense pressure on available water resources. The escalating requirements for water in different sectors, such as agriculture, industry, and domestic use, have created a situation where the water demand exceeds the available supply. Accurately quantifying the various components of the water budget is a crucial step in addressing the challenges of water resource management in the Awash River Basin. This information will provide valuable insights into the availability, distribution, and utilization of water resources at both sub-basin and basin scales. It will enable informed decision-making and promote sustainable socioeconomic development in the area.

Estimating water budgets has been extensively researched in various basins around the world, including Ethiopia. These studies focus on the availability, use, and management of water, in addition to the impacts of human activities and climate change on water resources. Techniques such as hydrological modeling, remote sensing, and data analysis are employed to estimate precipitation, evapotranspiration, runoff, and groundwater recharge. [3-24]. These studies significantly contribute to understanding the regional and temporal variability in water resources through water budget estimation at the basin scale. This aids in the formulation of water management strategies and policies. Furthermore, they enhance our comprehension of the impacts of climate change on the sustainability and availability of Ethiopia's water resources.

Water budget calculations are traditionally performed on a lumped scale, potentially leading to inaccurate estimates of water volume in specific hydrological components. To address this limitation, it is essential to develop a methodology that simulates the distribution of available and required water in a basin. This involves considering the assumptions and constraints of representative water budget models applied globally. Such a methodology plays a critical role in supporting decision-making processes aimed at ensuring the sustainable management of water resources [25]. This study does not encompass every model discussed in the literature but instead selectively focuses on models based on specified criteria. These criteria ensure the selected models are apt for accurately estimating water availability and fluxes within a specific context. By adhering to these criteria, stakeholders can easily identify the most fitting water budget model for their needs, facilitating informed decisions regarding water conservation and management. High spatial resolution grid-based water budget modeling presents challenges and requires extensive data. In contrast, semi-distributed water budget models demand minimal data and offer a simplified modeling approach, making them essential for effective and sustainable water resource management. This research employs daily hydro-meteorological data to develop a spatially semi-distributed water budget model at a sub-basin level. Focused on the economically and socially crucial upper awash sub-basin, the study utilizes a hydrologic model grounded in geographic information systems (GIS) to calculate groundwater recharge, surface runoff, and evapotranspiration. These calculations are based on variables such as land use, soil texture, topography, and hydro-meteorological data.

The objectives of the study are as follows:

- To assess the water budget components for 28 years.
- To assess the water budget components in different land use land cover (LULC) categories.
- To assess the Soil and Water Assessment Tool (SWAT) model's suitability for this study area.

2. Materials and Methods

2.1. Description of the Study Area

The Upper Awash River sub-basins, spanning 11,697 km^2, are situated in the central region of Ethiopia (Figure 1). The principal river, the Awash, extends over 178,411 km. Its significant tributaries include the Akaki and Mojo Rivers. The sub-basin's average elevation is approximately 2152 meters above sea level (masl), with an average slope of about 7.5%. The highest elevation point, located southwest of the area, reaches 3557 masl, whereas the lowest point, at the outlet of the Koka dam, is at 1579 masl. Nearly 84.6% of the watershed's area lies below 2500 m, and only 1.24% exceeds 3000 m in elevation. From 1986 to 2013, the average daily discharge at Hombele and Melkakuntiro was 43.77 and 29.52 cubic meters per second (m^3/sec), respectively, with the minimum values recorded at 0.401 and 0.173 m^3/sec and the maximum values at 803.1 and 555.12 m^3/sec.

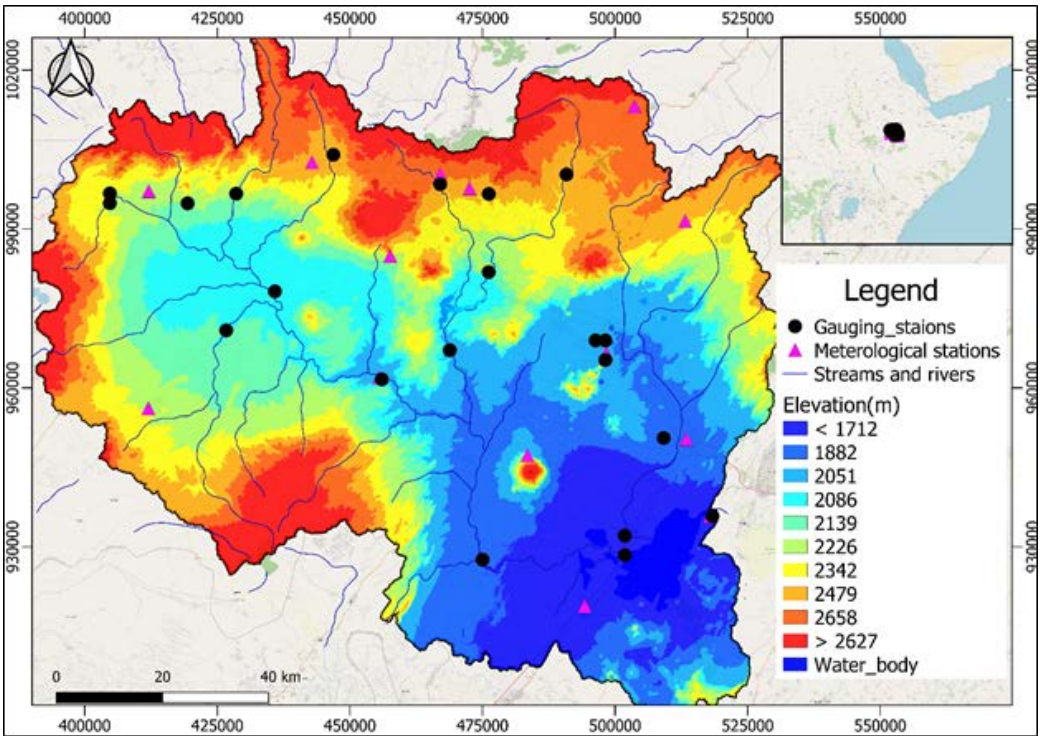

Figure 1: Location and Elevation Map of the Study Area.

Citation: Muauz, A., Berehanu, B., Bedru, H. (2024). Spatial Analysis of Water Budget Components in the Upper Awash River Sub-basin, Ethiopia Using SWAT Model. Journal of Earth & Environmental Waste Management. 2(3), 1-23.

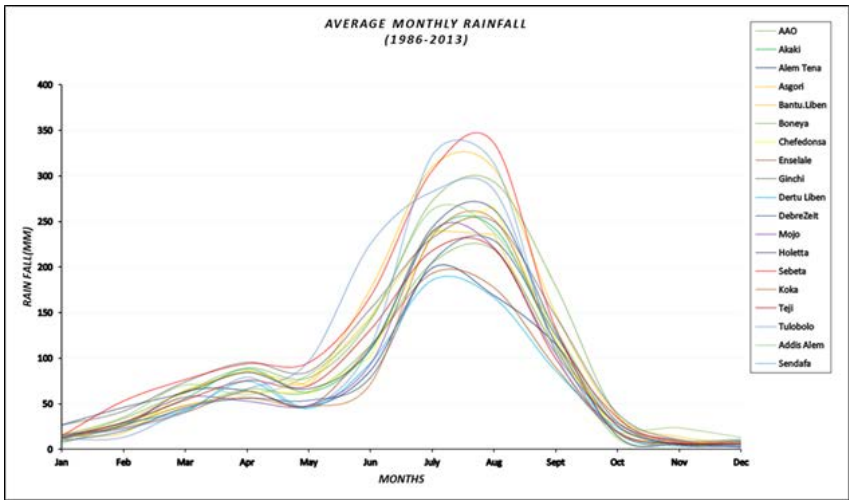

Figure 2: Mean Monthly Rainfall in the Upper Awash Sub-Basin.

The mean annual precipitation in the sub-basin is 1078 mm, with the lowest values observed in Debrezeit and the highest around Sebeta. Rainfall distribution is highly variable, both temporally and spatially, decreasing from the northwest to the southeast. The mean annual monthly precipitation data for the Upper Awash sub-basin is illustrated in Figure 2.The sub-basin's mean annual potential evapotranspiration, calculated using Thornthwaite's method from 1948, is approximately 1645 mm, with actual evapotranspiration being 859 mm. The average annual temperature in the sub-basin is 18.6 °C, ranging from about 16.4 °C to 21.8 °C. The lowest mean temperature, 5.2°C, occurs in January, while the highest average temperatures are recorded in April and May. In comparison to precipitation, temperature variations across the sub-basin are less pronounced.

The litho-stratigraphic units of the sub-basin are notably characterized by Tertiary-Quaternary volcanic rocks, covering a substantial area. Additionally, there are recognized occurrences of minor inter-trappean sediments, Quaternary lacustrine sediments, and surface deposits. The primary groundwater reservoirs are found within fractured regions of volcanic rock. The flowchart depicted in Figure 3 outlines the overall methodology for the study area.

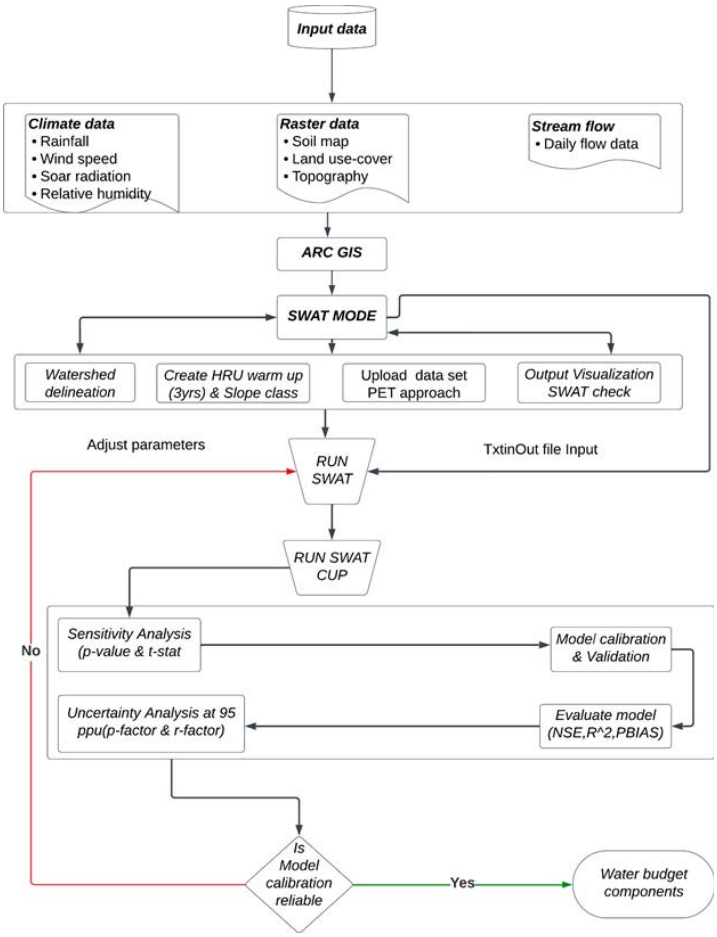

Figure 3: A Flowchart to Describe the Methodology

Citation: Muauz, A., Berehanu, B., Bedru, H. (2024). Spatial Analysis of Water Budget Components in the Upper Awash River Sub-basin, Ethiopia Using SWAT Model. Journal of Earth & Environmental Waste Management. 2(3), 1-23.

2.2. Model Description

SWAT, a semi-distributed, time-continuous watershed simulator, operates on a daily time step [26]. Developed to assess the impact of management practices and climatic conditions on water supplies, silt, and agricultural chemical yields in watersheds and larger river basins, SWAT distinguishes itself by its ability to capture a high level of spatial detail [26]. This is achieved by dividing the entire watershed into smaller sub-watersheds, each representing a distinct area within the larger watershed. Such an approach enables the model to more accurately represent the spatial variability of water availability and fluxes throughout the watershed. The main elements of SWAT include hydrology, weather, erosion, plant growth, nutrients, pesticides, land management, and stream routing, as outlined by [27]. Additionally, the software features an interface in ArcView GIS, which allows for the definition of watershed hydrologic features and storage, as well as the organization and manipulation of the associated spatial and tabular data [28].

By dividing the watershed into sub-basins, the study represents the area's large-scale geospatial heterogeneity. Within each sub-basin, hydrologic response units (HRUs) are identified based on distinct soil and land-use combinations. A weighted average approach aggregates various factors for each HRU within a sub-basin, including soil water content, surface runoff, nutrient cycles, sediment yield, crop growth, and management techniques. The physical characteristics of each sub-basin, such as slope, reach dimension, and meteorological information, are carefully considered. The SWAT model selects climate data from the station closest to the centroid of each sub-basin. This data informs the configuration of the river system, using the calculated flow, sediment yield, and nutrient loading for each sub-basin. Channel routing is simulated using either the Muskingum method or variable storage.

To approximate the water budget for each HRU, four storage volumes are considered: snow, soil profile, shallow aquifer, and deep aquifer. Surface runoff from daily rainfall is estimated using a modified SCS curve number approach, which accounts for local land use, soil type, and antecedent moisture condition. Peak runoff forecasts employ a modified version of the Rational Formula [29]. The watershed concentration time, incorporating both channel and overland flow, is calculated using Manning's formula.

The soil profile is divided into several layers, facilitating soil water processes such as infiltration, evaporation, plant uptake, lateral flow, and percolation to the lower layer. The soil percolation component of SWAT, which employs a water storage capacity approach, is used to forecast flow across each soil layer in the root zone. Downward flow occurs when a soil layer's field capacity is exceeded, provided the layer below is not saturated. Percolation from the base of the soil profile recharges the shallow aquifer. The simulated daily average soil temperature is determined by the maximum and minimum air temperatures. Percolation from a layer is prohibited if the temperature falls to zero degrees Celsius or below. Percolation and lateral sub-surface flow in the soil profile are estimated simultaneously. The contribution of groundwater flow to total streamflow is simulated by routing a shallow aquifer storage component to the stream [30]. Additionally, the model includes a mechanism for calculating discharge from frozen soil, where snow melts on days when the surface temperature exceeds a predetermined threshold, treating melted snow similarly to rainfall for runoff and percolation calculations.

The model distinguishes between soil and plant evaporation when calculating these processes. Potential evapotranspiration can be modeled using the Penman-Monteith, Priestley-Taylor, or Hargreaves methods [31-33]. This study employs the Penman-Monteith method, which requires inputs of solar radiation, air temperature, wind speed, and relative humidity. Potential soil water evaporation estimates are based on potential evapotranspiration and leaf area index. Actual soil evaporation is estimated using exponential relationships between soil depth and water content. The potential evapotranspiration, leaf area index, and root depth are utilized to model plant water evaporation, which may be limited by the soil's water content. The model is elaborated in [30].

Model equations are available in the SWAT theoretical documentation and on the SWAT model website. An overview of climatic inputs and the hydrologic balance of Hydrologic Response Units (HRUs), cropping and management inputs and HRU-level pollution losses, and flow and pollutant routing is provided in [30, 34].

2.3. Input Parameters

Through the ARCSWAT interface, the 2012 version of SWAT was employed for computational simulation. SWAT, a physically based model designed to simulate complex hydrological processes, requires extensive detailed information about the basin, including topography, land use, soil properties, and meteorological data [26]. These data were collected from various sources and databases, as summarized in Table 1, providing the minimum necessary information for the SWAT model.

For watershed delineation, the SWAT watershed delineator tools utilize Digital Elevation Model (DEM) data. In this study, DEM data from the Shuttle Radar Topography Mission (SRTM) of the USGS, with a resolution of 30 m by 30 m, was used. The study area's elevation ranges from 1579 to 3564 meters above sea level (masl), with the highest points located in the southwest part of the area and the lowest at the Koka dam outlet, as depicted in Figure 1.

Figure 4 illustrates the distribution of land slope classes in the Upper Awash basin. The results indicate that the most common slope category, covering 41.1% of the area, is the 0-5% slope class. Slopes ranging from 5-10% constitute the second most prevalent class, accounting for 31% of the total area. Additionally, 18.9% of the area features slopes between 10 and 20%. A smaller portion, 5.32% of the area, falls within the 20-30% slope class. Lastly, 3.68% of the area has slopes exceeding 30%, highlighting significant topographic variability within this region of the Upper Awash basin.

Citation: Muauz, A., Berehanu, B., Bedru, H. (2024). Spatial Analysis of Water Budget Components in the Upper Awash River Sub-basin, Ethiopia Using SWAT Model. Journal of Earth & Environmental Waste Management. 2(3), 1-23.

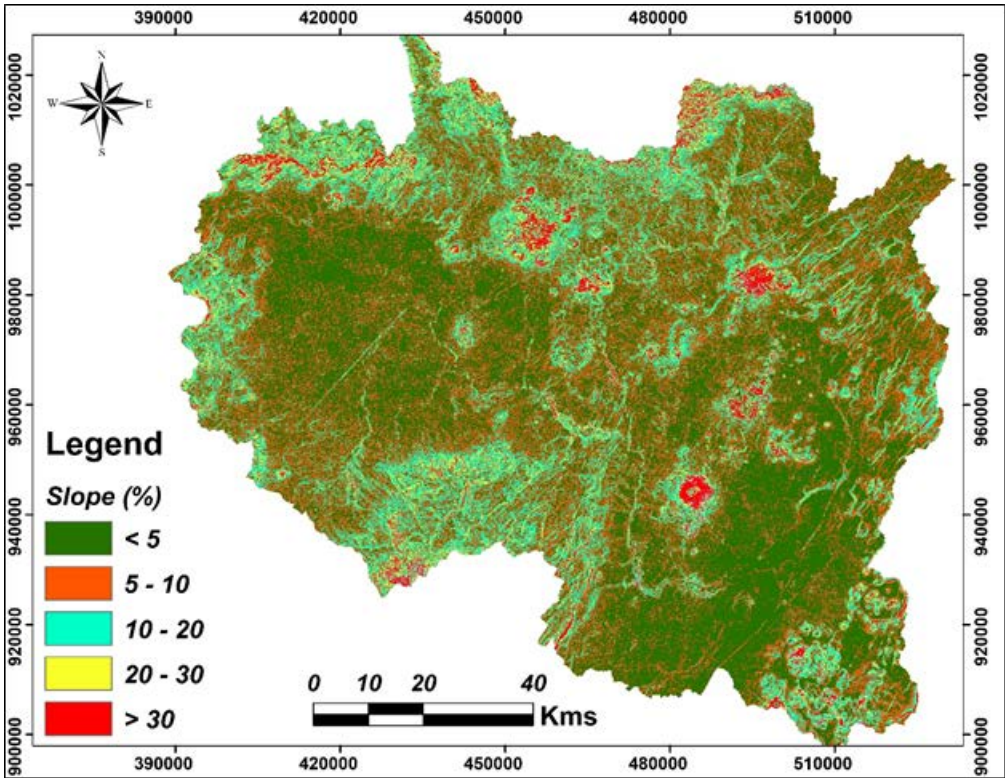

Figure 4: Slope Classification

The computer simulation was conducted using the ArcGIS 10.2.2 ARCSWAT interface, paired with SWAT version 2012 [26]. The physically-based SWAT model requires extensive detailed data about the basin to accurately simulate complex hydrological processes. Necessary data for the SWAT model, including topography, land use, soil qualities, and meteorological data, were collected from various sources and databases. These data and their sources are summarized in Table 1.

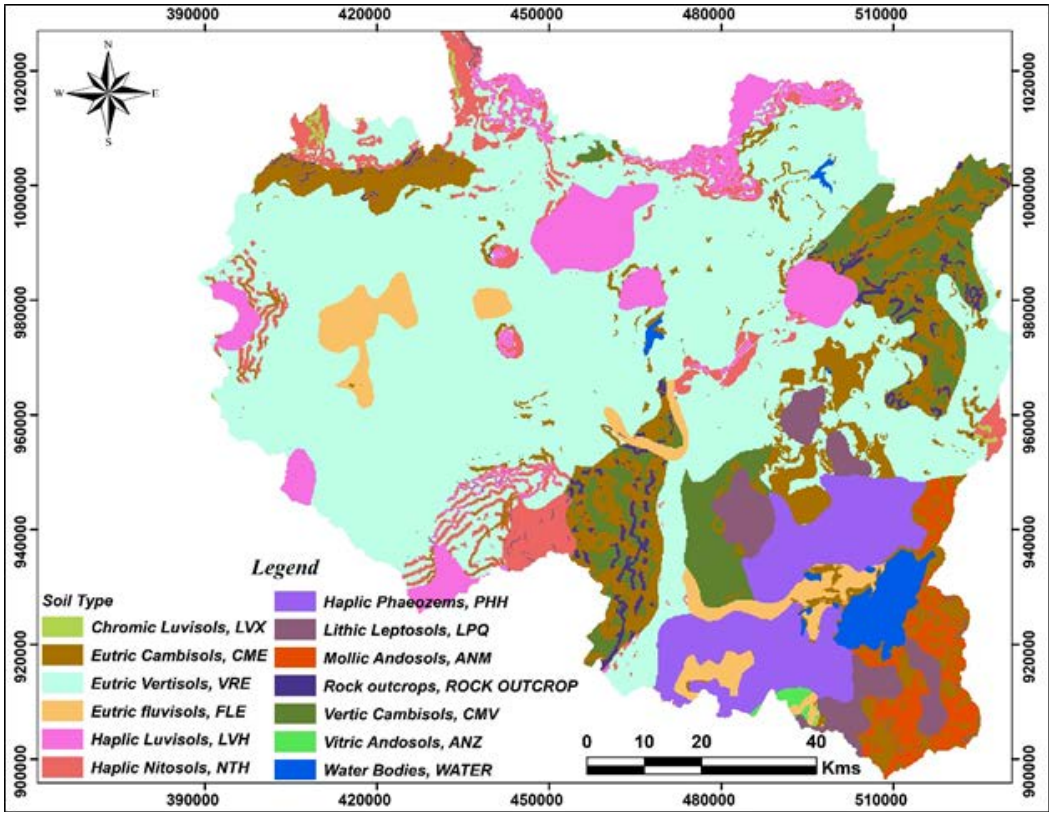

Figure 5: Soil Distributed Map

Citation: Muauz, A., Berehanu, B., Bedru, H. (2024). Spatial Analysis of Water Budget Components in the Upper Awash River Sub-basin, Ethiopia Using SWAT Model. Journal of Earth & Environmental Waste Management. 2(3), 1-23.

Table 1: The available data set for setting the SWAT model

Sn	Spatial data	Description	Source
1	Digital Elevation Model	30 m×30 m grid DEM has been used to delineate the boundary of the watershed and analyze the drainage patterns of the terrain.	Shuttle Radar Topography Mission (SRTM) of USGS
2	Land use and land cover	Africa land use 2013	Ethiopian Map Agency
3	Soils data	The soil data has been obtained from FAO	Ministry of Agriculture, Government of Ethiopia
4	Weather data	All-weather parameters	Ethiopian Meteorological Agency
5	Hydrological data	Gauge data in the study area gauge station	Ministry of Water, Irrigation and Energy, Government of Ethiopia

Soil physicochemical and hydrological properties were obtained from various FAO-UNESCO soil databases [35]. These databases provide attributes for each soil polygon, including soil texture, hydrological soil group (HSG), soil depth, rock fragments, and organic carbon content. They are considered the most comprehensive resource available, offering an extensive database of soil attributes for Africa and the world (historic report). Table 2 presents the cover area and percentage distribution of twelve soil groups in the study area watershed, providing a detailed understanding of soil composition and distribution. The spatial distribution of soils is depicted in Figure 5.

Agricultural activities utilize 69.1% of the land in the basin, predominantly arable fields. Forests account for approximately 5.4% of the total land area. As shown in the land use cover map (Figure 6), the remaining area is occupied by urban regions, surface waters, and barren land.

Table 2: Characteristics of the Modelled Upper Awash Sub-Basin

Parameter	Type/class	Area (km^2)	Basin area (%)
LANDUSE	Agricultural Land Generic (AGRL)	8077	69.09
	Range-Grasses (RNGE)	2408	20.60
	Forest-Evergreen (FRSE)	625	5.35
	Residential (URBN)	394	3.37
	Water body(WATR)	164	1.40
	Range-Brush (RNGB)	15	0.13
	Wetlands(WETF)	8	0.07
SOIL	Haplic Nitosols (NTH)	606	5.13
	Lithic Leptosols (LPQ)	393	3.33
	Chromic Luvisols (LVX)	22	0.19
	Haplic Luvisols (LVH)	796	6.75
	Eutric fluvisols (FLE)	438	3.71
	Vertic Cambisols (CVE)	656	5.56
	Rock outcrops	142	1.20
	Haplic Phaeozems (PHH)	811	6.87
	Vitric Andosols (ANZ)	19	0.16
	Mollic Andosols (ANM)	251	2.13
	Eutric Vertisols (VRE)	5878	49.81
	Eutric Cambisols (CME)	1596	13.53
SLOP (%)	< 5	4804.03	41.1
	5_10	3623.96	31
	10_20	2209.13	18.9
	20_30	621.74	5.32
	> 30	430.43	3.68

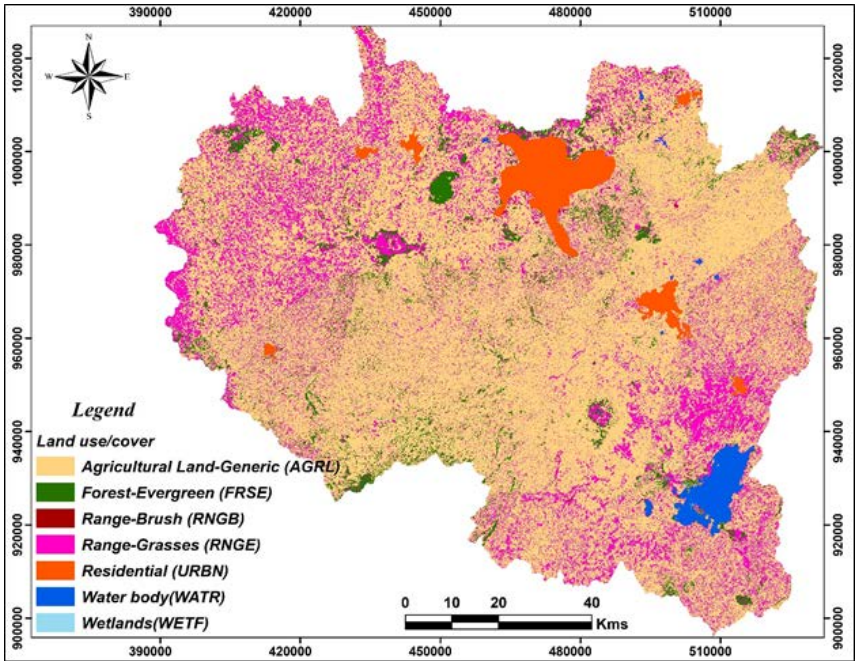

Figure 6: Land use/ Cover Map (Ethiopian Land Cover Map 2013)

2.4. Sensitivity Analysis

Calibration is essential for optimizing model parameters to reduce uncertainty in model outputs. Determining which parameters to calibrate is challenging in models with multiple parameters. Sensitivity analysis plays a crucial role in identifying and ranking parameters that significantly impact the desired model outputs [36].

The SWAT Calibration and Uncertainty Programs (SWAT-CUP) utilize the Sequential Uncertainty Fitting Version 2 (SUFI2) technique to assess the sensitivity of SWAT parameters. This process carried out alongside the calibration procedure, requires the inclusion of SWAT-estimated and monitored flows. The necessity arises because the objective function, which evaluates the success of model calibration, bases its sensitivity estimates on fluctuations.

Table 3: Parameters Considered in the Sensitivity Analysis

Parameter name	Description
CN2	SCS runoff curve number
ESCO	Soil evaporation compensation factor
GWQMN	Threshold depth of water in the shallow aquifer required for return flow to occur (mm H2O)
SOL_AWC	Soil available water storage capacity (mm H2O/mm soil)
GW_REVAP	Groundwater revap coefficient
SOL_Z	Soil depth (mm)
SURLAG	Surface runoff lag coefficient (days)
SOL_K	Soil conductivity (mm/h)
CH_K2	Effective hydraulic conductivity in the main channel (mm/h)
ALPHA_BF	Baseflow alpha-factor (days)
GW_DELAY	Groundwater delay (days)
REVAPMN	Threshold depth of water in the shallow aquifer for “revamp” to occur (mm)
CH_K2	Effective hydraulic conductivity in main channel alluvium (mm/hr)
OV_N	Manning’s n value for overland flow
CH_N2	Manning’s coefficient for channels
BIOMIX	Biological mixing efficiency

Equation.1, which provides the values of the parameters obtained by the Latin hypercube sampling vs the objective function values, is used to calculate the sensitivity of the parameters [37].

$$g = \alpha + \sum_{i=1}^{m} \beta_i b_i \quad \text{Equation.....1}$$

Where g is the objective function value; b is the parameter; α is the regression constant; β corresponds to the technical coefficient attached to the variable b, and m is equal to the number of parameters.

The variance mean of the goal function calculates the sensitivity by changing each parameter individually while keeping the other parameters constant. Sensitivity is assessed using the t-statistic (t-stat) and the p-value. A parameter is considered more sensitive when the absolute value of the t-stat is higher and the p-value is smaller [37]. Sensitivity analysis begins by selecting parameters based on their t-stat and p-value. Following this analysis, model calibration is performed using the parameters identified as most sensitive. These parameters are detailed in Table 3 as the final parameters for the study.

The t-stat is calculated by dividing a parameter's regression coefficient by its standard error. A parameter is deemed sensitive if its coefficient value exceeds its standard error and the t-stat is greater than zero [38]. The p-value is calculated by comparing the t-stat to the values in the t-Student distribution table, testing the null hypothesis that the regression coefficient equals zero.

The analysis utilizes variables that affect a river basin's water output, which can be modified. These parameters are listed in the SWAT database, including their value ranges, the action plan (basin, sub-basin, or HRU), the type of value variation (specific value replacement, addition to the existing parameter value, or multiplication of an existing parameter value), and the sensitivity-analysis group (water production, sediment yield, or water quality).

2.5. Uncertainty Analysis

Hydrological modeling necessitates an uncertainty analysis to quantify and understand the uncertainties inherent in model predictions. This analysis primarily involves the r-factor and p-factor, which reveal uncertainties in peak flows and volume predictions, respectively.

The r-factor is the ratio of the simulated to the observed volume of flow, assessing the uncertainty associated with the magnitude of flow predictions. A low r-factor signifies a good agreement between simulated and observed volumes, indicating lower uncertainty. Conversely, a high r-factor indicates a significant discrepancy between the simulated and observed volumes, suggesting higher uncertainty in the model predictions.

The p-factor, in contrast, is the ratio of the simulated to observed peak flows. It evaluates the uncertainty associated with the timing of peak flows. Like the r-factor, a low p-factor denotes a good agreement between the simulated and observed peak flows, suggesting lower uncertainty. A high p-factor, however, indicates a significant discrepancy in the timing of peak flows, implying higher uncertainty in the model predictions.

Our assessment of the reliability and accuracy of hydrological models involves analyzing these factors in uncertainty analysis. The r-factor and p-factor are instrumental in identifying potential sources of uncertainty by measuring the agreement between observed and simulated flow characteristics.

2.6. Model Calibration and Validation

The first step in calibrating a traditional watershed model involves dividing the measured streamflow time series into two segments: calibration and validation. During the calibration period (1988–2008), model inputs across the basin are adjusted until the simulated flow closely matches the observed flow at the basin outlet. Following calibration, the model is run for the validation period (2009–2013) using the same input parameters. The goodness-of-fit is then evaluated. Model validation aims to determine whether the calibrated model can accurately predict streamflow for subsequent periods, using the same parameters, without necessitating further adjustments that were made during the calibration phase.

2.7. Model Performance Evaluation

To assess the model's behavior, the p-factor and r-factor were utilized to estimate the goodness of uncertainty performance. The p-factor represents the proportion of data covered by the 95PPU (with a maximum value of 100%), while the r-factor signifies the average width of the band divided by the standard deviation of the corresponding measured variable. The performance of the SWAT model was statistically evaluated using the coefficient of determination (R^2), the Nash-Sutcliffe efficiency (NSE), and the percent bias (PBIAS). These statistical criteria were computed using the SUFI-2 approach.

The coefficient of determination (R^2) illustrates the model's percentage of variation in measured data, indicating the magnitude of the linear relationship between the simulated and observed values. Higher numbers suggest less error variance, with values larger than 0.6 generally considered acceptable. R^2 ranges from 0, indicating a poor model, to 1, indicating a good model [39]. Equation 2 can be used to determine the value of R^2.

$$R^2 = \left[\frac{\sum_{i=1}^{n}(O_i - S_i)(S_i - \bar{S})}{(\sum_{i=1}^{n}(O_i - \bar{O})^{0.5})(\sum_{i=1}^{n}(S_i - \bar{S})^2)^{0.5}}\right]^2 \quad \text{Equation.....2}$$

Where, O_i – measured value (m3/s)
$\bar{O}$ – Average measured value (m3/s)
S_i – Simulated value (m3/s) and
S – Average simulated value (m3/s)

The Nash-Sutcliffe efficiency (NSE), a normalized statistic, assesses how much residual variation (additionally recognized as "noise") there is about the variance of the

measured data (also known as "information") [40]. NSE represents how well the 1:1 line fits the observed versus simulated data plot. NSE is calculated as the equation indicates. 3:

$$NSE = 1 - \left[\frac{\sum_{i=1}^{n}(OO_{ii} - S_I)^2}{\sum_{I=1}^{n}(O_I - \overline{Oi})^2}\right] \text{ Equation .....3}$$

NSE has a value between negative infinity and one (best), or [-, 1]. NSE value 0 denotes poor performance because it shows that the mean observed value is a better predictor than the simulated value. While NSE values greater than 0.5, the simulated value is a better predictor than the mean measured value and is generally viewed as an acceptable performance [39].

The average tendency of the simulated data to be greater or smaller than their observed equivalents is represented by percent bias [40, 41]. Low-magnitude values of PBIAS indicate accurate model simulation, with 0.0 being the ideal value. Positive values denote a bias in the model's underestimation, whereas negative values denote a bias in the model's overestimation [41]. Using the equation 4, PBIAS is calculated.

$$PBIAS = \left[\frac{\sum_{n=1}^{n}(O_I - S_i) * 100}{\sum_{ii=1}^{n}(O_i)}\right] \text{ Equation } \ldots\ldots\ldots\ldots\ldots 4$$

Where PBIAS is the deviation of data being evaluated, expressed as a percentage.

2.8. Water budget components

The simulated annual water budget components refer to the various inputs and outputs of water in a given area over the course of a year. These components can include precipitation, evapotranspiration, surface runoff, infiltration, and groundwater recharge. To better understand the water budget in a particular area, it is often helpful to examine the ratio of rainfall amounts to each of the water budget components. This can provide insight into how much of the precipitation is used by vegetation, how much is being lost to evaporation, and how much contributes to groundwater recharge or surface runoff. For example, a high ratio of rainfall to evapotranspiration may indicate that the area is heavily vegetated and that much of the precipitation is used by plants. On the other hand, if the ratio of rainfall to runoff is low, it may suggest that the area is experiencing drought conditions and that little precipitation is making its way into rivers or other surface water bodies. The number of inputs and outputs of water in a specific area was calculated using a mathematical formula known as the water budget equation. Hydrologists, water resource managers, and other experts frequently use it to comprehend the water budget in a particular watershed or area. The water budget equation considers a variety of water inputs into an area, such as precipitation and groundwater recharge, and a variety of water loss mechanisms, such as evaporation, transpiration, and surface runoff.

The general form of the water budget equation is:

$$P = ET + Q + \Delta S \text{ Equation.....5}$$

Where P represents precipitation, ET represents evapotranspiration, Q represents runoff, and ΔS represents the change in storage of water over time.

Surface runoff: The estimation of surface runoff in this study is based on a modification of the SCS-CN method developed by [42]. Surface runoff refers to the excess water that flows overland after infiltration and depression storages are filled. The SCS-CN method considers various factors such as antecedent moisture conditions, infiltration, soil type, land cover, and topography to estimate surface runoff.

The SCS-CN method used in this study is defined as per [42]. To estimate surface runoff from storm rainfall, the Soil Conservation Service (USDASCS, 1972) equation is used, which is as follows:

$$Q = \frac{(P - 0.2S)^2}{(P + 0.8S)} \text{ Equation.....6}$$

$$S = \frac{25400}{CN} - 254 \text{ Equation .....7}$$

Where Q is the surface runoff (mm), P is the precipitation (mm), and S is the potential maximum retention after runoff begins (mm). The value of S is a function of the soil type and land cover in the area. CN is a dimensionless curve number that depends on the type of land used, the hydrological soil group, and the preexisting moisture conditions II (i.e., the soil is near field capacity).

Evapotranspiration: Evapotranspiration is the process of water loss through evaporation and transpiration. It is a crucial component of the water balance equation and plays a significant role in the hydrological cycle. However, the estimation of evapotranspiration is a challenging task and often subject to significant uncertainty.

The FAO56PM model is widely used to estimate reference crop evapotranspiration, as developed by as follows in equation 8. This model considers various factors such as temperature, humidity, solar radiation, and wind speed to estimate reference crop evapotranspiration. Reference crop evapotranspiration is defined as the rate of evapotranspiration from a well-watered reference crop, such as grass or alfalfa, under standard environmental conditions [43].

$$ET = \frac{0.408\Delta(R_n - G) + \gamma\frac{900}{Ta+273}u_2(e_s - e_a)}{\Delta + \gamma(1 + 0.34u_2)} \text{ Equation } \ldots\ldots\ldots\ldots\ldots\ldots 8$$

ET stands for reference crop evapotranspiration (mm/d), γ for the psychrometric constant (kPa/°C), R_n for net solar radiation at the crop surface (MJ/m2/d), G for soil heat flux (MJ/m2/d), Δ is the slope of saturation vapour pressure versus air temperature curve (kPa/°C)Ta for the mean air temperature at 2m height (°C), u2 for wind speed at 2m height (m/s), e_s for saturation vapour pressure (kPa), and e_a for actual vapour pressure (kPa). The water budget in each cell is to be computed using the derived runoff and actual evapotranspiration on an annual basis. To reduce complexity, the percolation and deep percolation components are not

taken into separate accounts when developing the model.

Groundwater recharge: Groundwater is a critical resource replenished through percolation and water movement through the vadose zone, ultimately recharging aquifers. The recharge rate is influenced by various factors, including the hydraulic properties of geological formations within the vadose zone and the water table [27]. This study utilized the exponential decay function proposed by to estimate groundwater recharge. This approach accounts for the vadose zone and water table properties to determine the volume of water entering the aquifer system [44]. The exponential decay formula is based on the premise that the recharge rate decreases exponentially as the distance from the recharge source increases. The method assumes the vadose zone is homogeneous and isotropic, a widely accepted notion critical for predicting groundwater recharge accurately.

3. Results and Discussion

3.1. Watershed Delineation

To accurately represent the complex hydrological processes in the study area, the watershed was segmented into 35 sub-basins. This segmentation was based on the digital elevation model (DEM) and the stream network. Within each of these sub-basins, the SWAT model further subdivided the landscape into 1,415 hydrological response units (HRUs). These HRUs were differentiated based on variations in land use, soil types, and slope gradients. This methodology facilitated a more precise representation of the spatial variability within the study area. Notably, the fluviometric station of Hombele was positioned in sub-basin Number 33, and Melkakuntro was located in sub-basin Number 20.

3.2. Sensitivity Analysis

The sensitivity analysis conducted in this study initially considered sixteen parameters to identify the most influential factors affecting streamflow in the study area. After analyzing the results, six parameters were found to have the lowest p-values and higher t-stat values, indicating their sensitivity to streamflow at both monitoring stations. The first parameter identified was the SCS runoff curve number (CN2), which represents the soil's ability to absorb water. This parameter is a critical factor in determining the amount of runoff generated during rainfall events. The second parameter, the alpha factor (ALPHA_BF), is largely responsible for the groundwater recharge rate. It measures the rate of water transfer from the surface to the groundwater system. The third parameter, the groundwater delay (GW_DELAY), represents the time it takes for water to move from the surface to the groundwater system. This parameter is crucial in determining when and how quickly groundwater recharges. The fourth parameter is the threshold depth of water in the shallow aquifer necessary for return flow to occur (GWQMN). This denotes the minimum amount of water needed in the shallow aquifer for water to return to the surface, as shown in Figures 7 and 8.

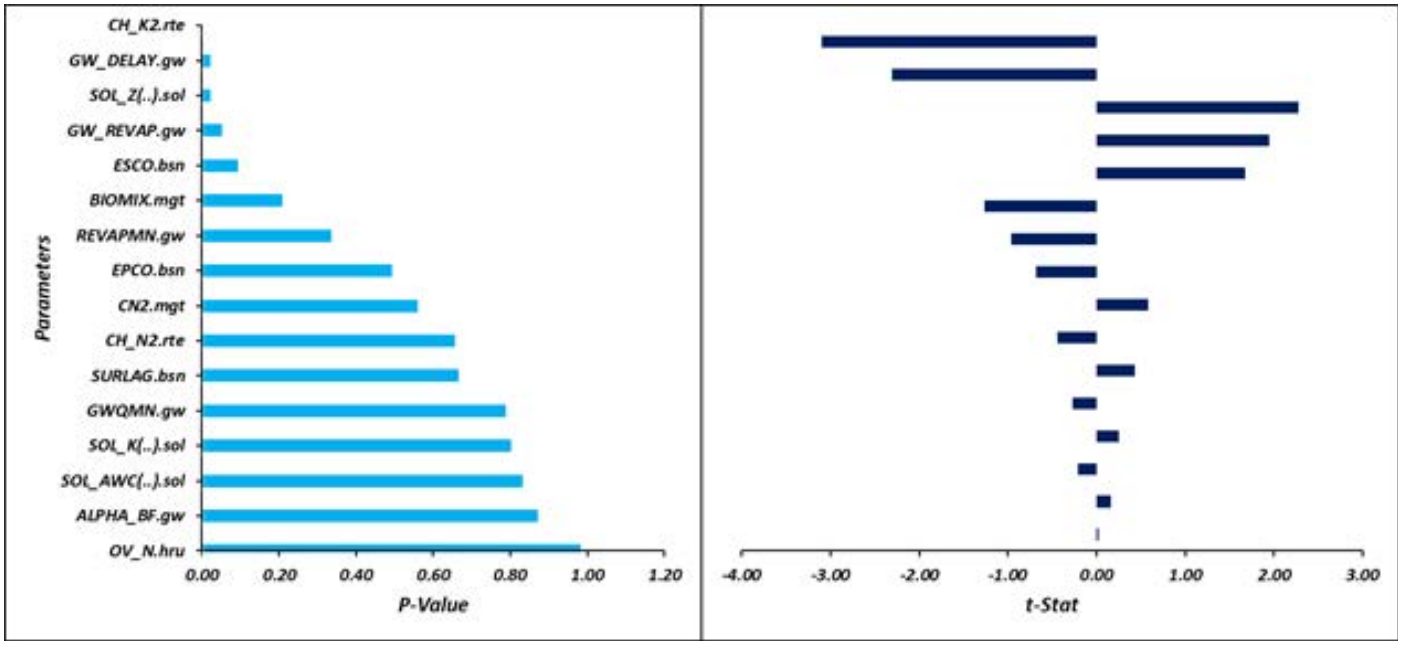

Figure 7: Sensitivity of Flow Parameters Hombele Gauging Station

Citation: Muauz, A., Berehanu, B., Bedru, H. (2024). Spatial Analysis of Water Budget Components in the Upper Awash River Sub-basin, Ethiopia Using SWAT Model. Journal of Earth & Environmental Waste Management. 2(3), 1-23.

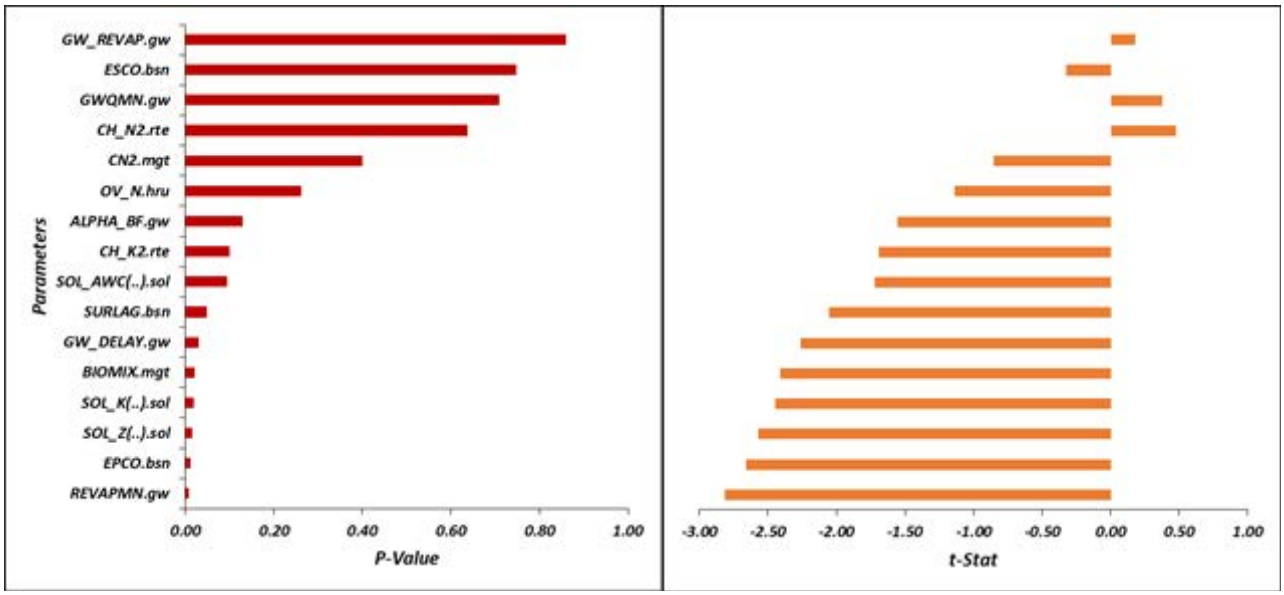

Figure 8: Sensitivity of Flow Parameters at Melkakuntiro Gauging Station

3.3. Calibration, Validation and Uncertainty Analysis

Table 4 presents the initial ranges and calibrated sensitive parameters for streamflow in the study area. It provides valuable information on the range of values for each parameter and the final calibrated values after sensitivity analysis. This information is crucial for understanding the factors that influence streamflow and for developing sustainable water resource management strategies. For the gauging stations at Hombele and Melkakuntiro, plots of the daily simulated and observed streamflow were made to assess the calibrated model's effectiveness. The results showed good agreement between the datasets, with Nash-Sutcliffe Efficiency (NSE) values of 0.82 and 0.78 and R2 values of 0.82 and 0.79 for the calibration period (1988–2008), respectively. For the validation period (2009–2013), the NSE and R2 values were 0.67 and 0.66, and 0.71 and 0.7, respectively (figure 9).

Table 4: Initial Ranges and Final Calibrated Sensitive Parameters

Parameter	Minimum	Maximum	Calibrated value
Alpha_Bf	0	1	0.048
Biomix	0	1	0.2
Ch_K2	0	150	0
Ch_N2	0	1	0.014
Cn2	35	98	71.2
Epco	0	1	1
Esco	0	1	0.95
Gw_Delay	0	50	31
Gw_Revap	0.02	0.2	0.02
Gwqmn	0	5000	1000
Revapmn	0	500	750
Sol_Awc	0	1	0.1
Sol_K	0	100	17.27
Sol_Z	0	3000	204.03
SURLAG	0	10	4
OV_N	0	0.8	0.14

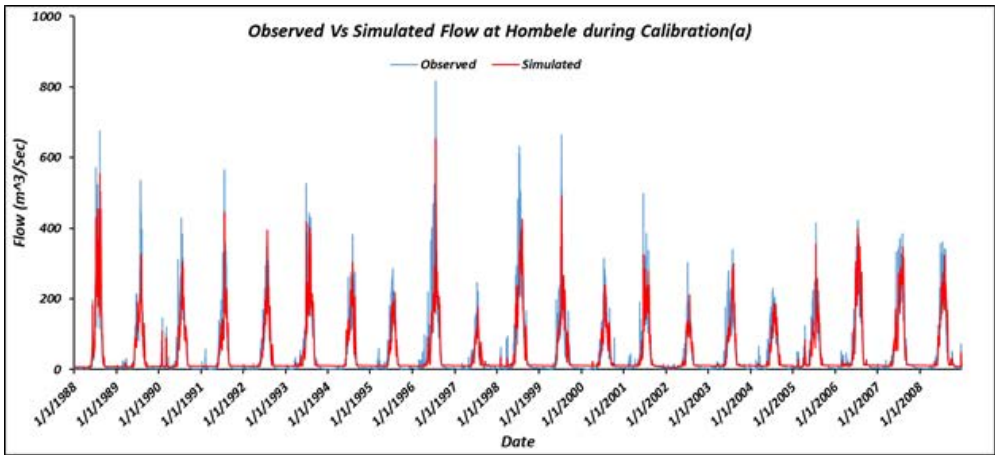

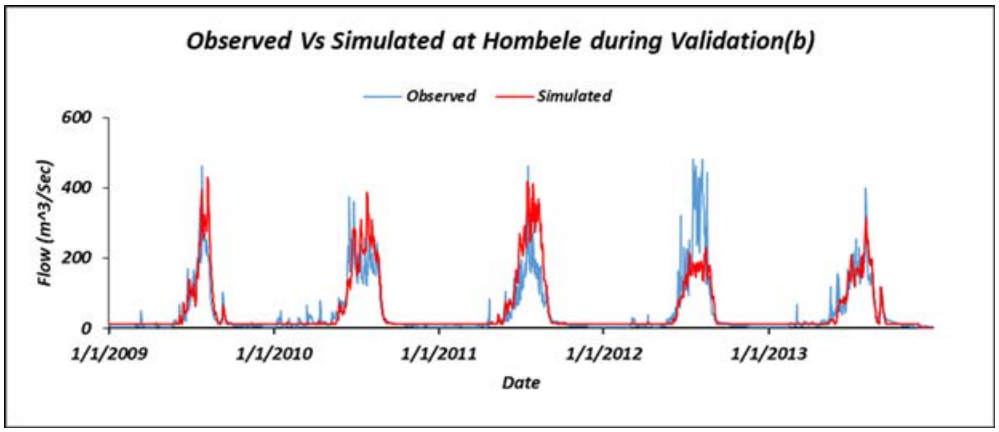

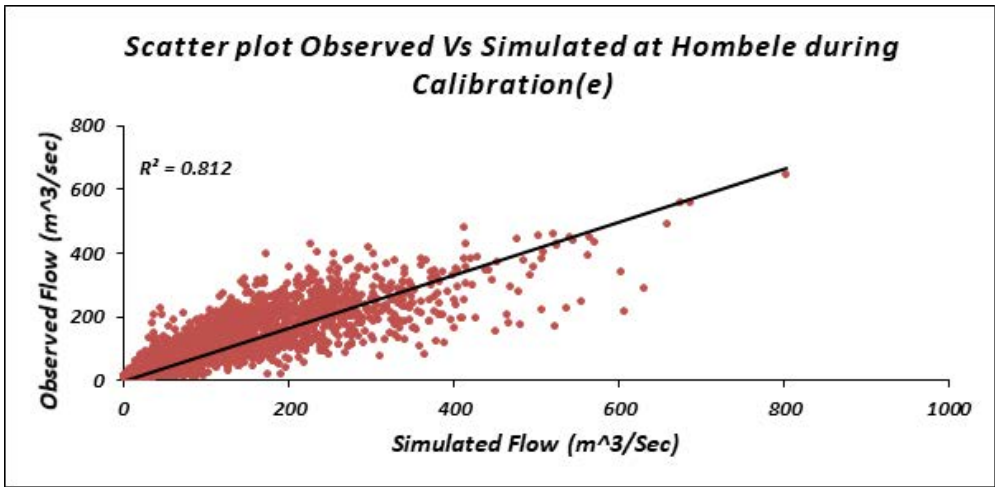

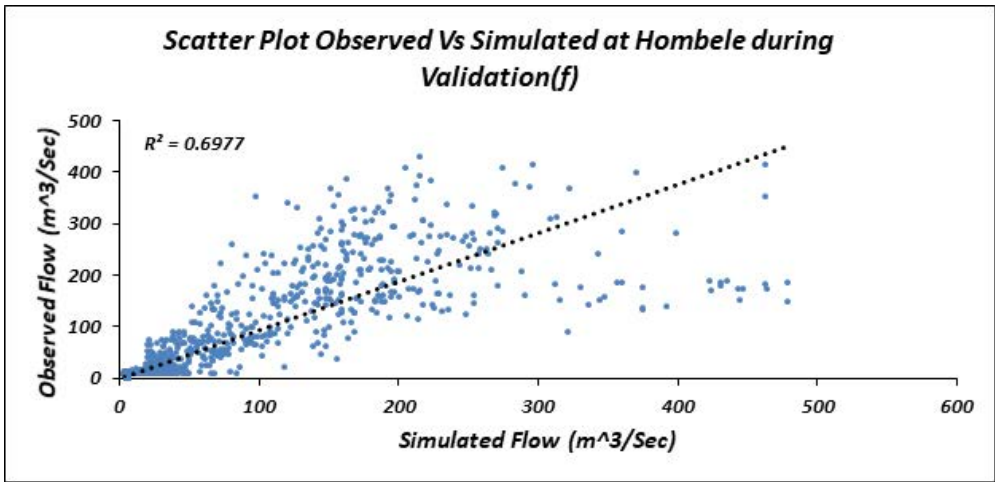

Citation: Muauz, A., Berehanu, B., Bedru, H. (2024). Spatial Analysis of Water Budget Components in the Upper Awash River Sub-basin, Ethiopia Using SWAT Model. Journal of Earth & Environmental Waste Management. 2(3), 1-23.

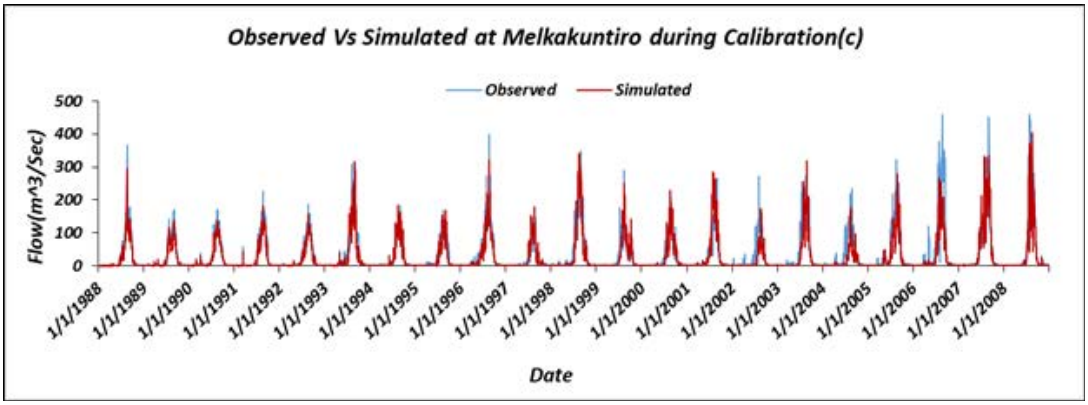

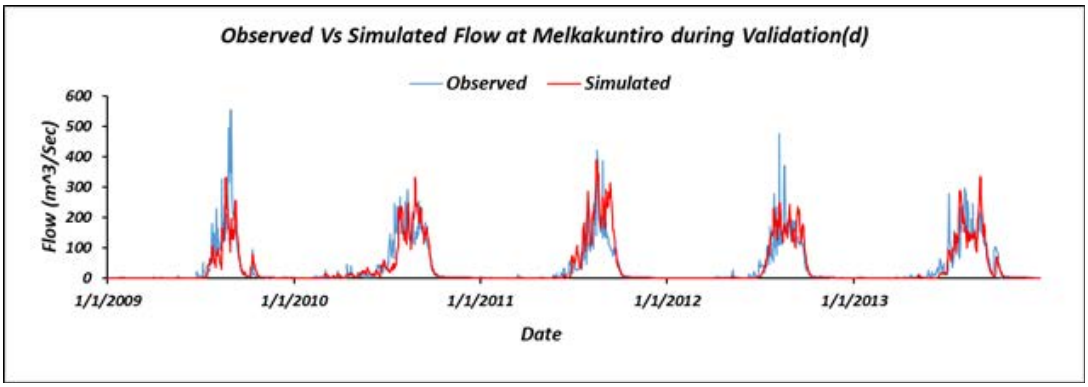

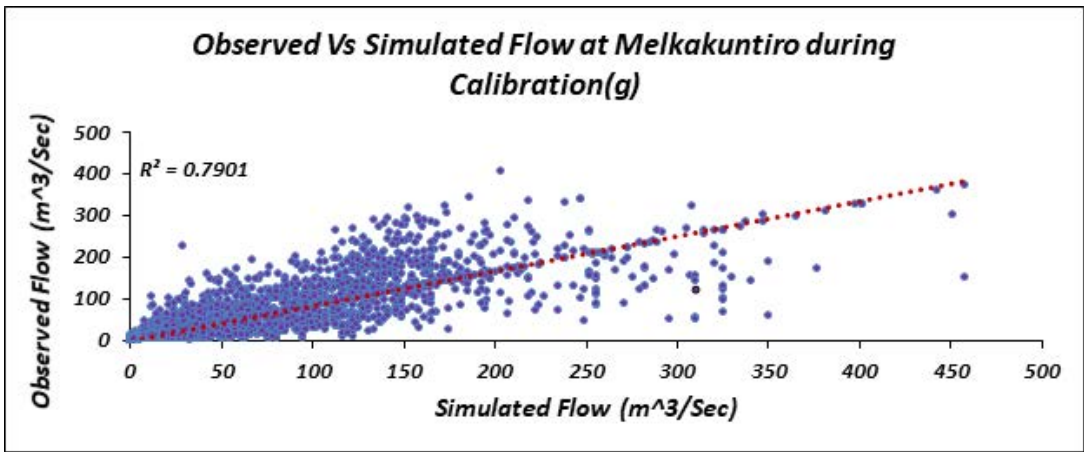

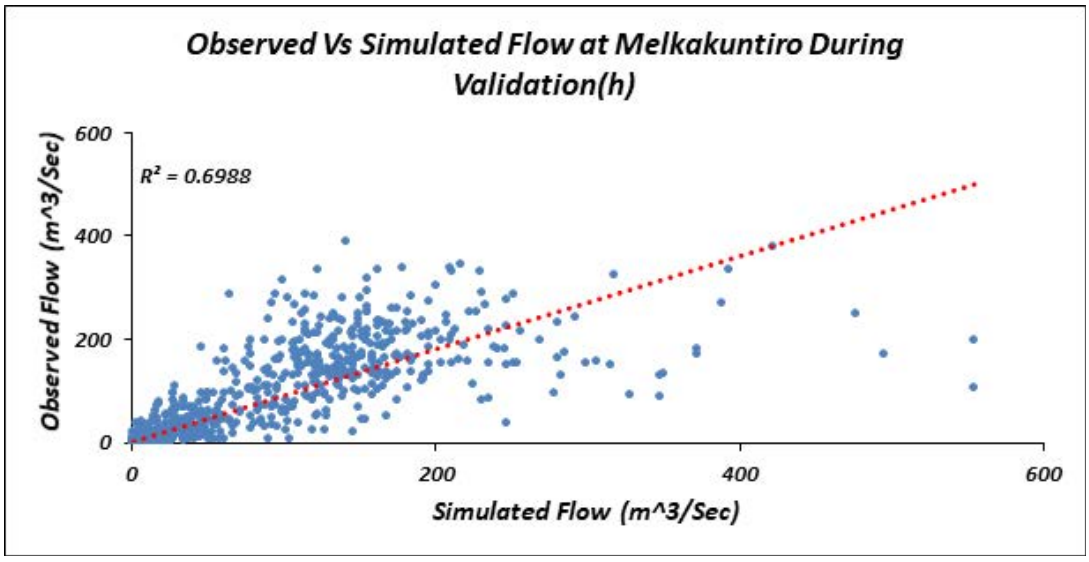

Figure 9: The Time Series Data for Hombele (a & b) and Melkakuntiro (c & d) are Depicted for both the Calibration and Validation Period and Scatter Plots Illustrate the Comparisons of Daily Streamflow between Simulated and Observed Data at Hombele (e & f) and Melkakuntiro (g & h) during the Calibration and Validation Processes.

Considering the model performance statistics for the calibration periods at Hombele and Melkakuntro stations, and based on the criteria set out by Moriasi et al. for assessing model performance, the setup model was rated as "very good" and "good" respectively shown in Table 5. For the validation periods, the ratings were "good". These model performance measures indicate that the model accurately captures the observed streamflow at the Hombele station. However, a comparison of the statistical measures for the calibration and validation periods reveals that the model performed better during the calibration period than during the validation period.

The observed and simulated discharges matched well during both the calibration and validation periods (Table 6). However, during the calibration periods at the Hombele and Melkakuntro gauging stations, there was an average underestimation of the observed discharge by 2.3% and 13.1%, respectively. During the validation period, there was an overestimation of the observed discharge by 11.2% at Hombele

and 1.9% at Melkakuntro. During the calibration period (1988–2008), the observed and simulated mean annual flow (MAF) were 1421 MCM/yr (45.03 m3/s) and 1389 MCM/yr (44.01 m3/s), respectively, indicating an underestimation of the observed streamflow by 2.3% at the Hombele station. The observed and simulated MAF at Melkakuntro were 943 MCM/yr (29.88 m3/s) and 819 MCM/yr (25.96 m3/s), respectively, representing a 13.1% underestimation of the observed streamflow. For the validation period (2009–2013), the observed and simulated flows (MAF) at Hombele and Melkakuntro were 1450 MCM/yr (45.95 m3/s), 1612 MCM/yr (51.08 m3/s), 1140 MCM/yr (36.13 m3/s), and 1160 MCM/yr (36.8 m3/s), respectively, resulting in an overestimation of the observed discharge by 11.2% and 1.9%.

Table 5: Classification of Statistical Indices

R^2	NSE	PBIAS	Classification
$0.75 < R^2 < 1.00$	$0.75 < NSE < 1.00$	$PBIAS < + 10$	Very Good
$0.60 < R^2 < 0.75$	$0.60 < NSE < 0.75$	$+ 10 < PBIAS < + 15$	Good
$0.50 < R^2 < 0.60$	$0.36 < NSE < 0.60$	$+ 15 < PBIAS < + 25$	Satisfactory
$0.60 < R^2 < 0.50$	$0.00 < NSE < 0.36$	$+ 25 < PBIAS < + 50$	Bad
$R^2 < 0.25$	$NSE < 0.00$	$+ 50 < PBIAS$	Inappropriate
Source: Adapted from Moriasi et al. (2007),			

Table 6: Performance Indexes

Performance Indexes	Gauging stations	PBIAS	Classification	
	Hombele		Melkakuntro	
	Calibration	Validation	Calibration	Validation
R2	0.82	0.71	0.79	0.7
NSE	0.82	0.63	0.63	0.66
PBIAS	2.3	-11.2	13.1	-1.9

In the case of Hombele, the p-factor and r-factor ratios during calibration were 0.801 and 0.97, respectively. This indicates that the model was able to reasonably simulate the peak flows and volume of flow, capturing approximately 80.1% and 97% of the observed values, respectively. Similarly, for Melkakuntro, the p-factor and r-factor ratios during calibration were 0.808 and 0.868, indicating a slightly lower but still acceptable level of performance (Table 7).

Table 7: Uncertainty Indexes

Uncertainty Indexes	Gauging stations	PBIAS	Classification	
	Hombele		Melkakuntro	
	Calibration	Validation	Calibration	Validation
p-factor	0.801	0.387	0.808	0.352
r-factor	0.97	0.9	0.868	0.98

3.4. Water Budget Components in the Upper Awash Sub-Basin

The components of a simulated annual water budget for the study area are shown in Figure 10. These elements include the annual amounts of precipitation, evapotranspiration, surface runoff, and groundwater recharge in the region. The annual rainfall in the study area is shown in Figure 11.

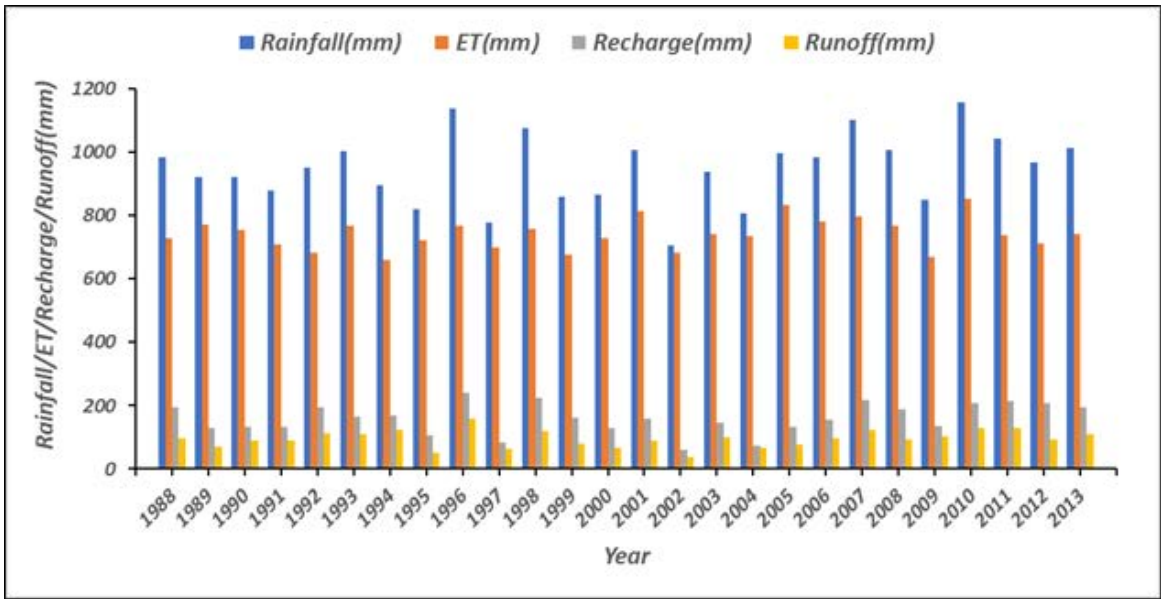

Figure 10: The Simulated Annual Water Budget Components in the Upper Awash Sub-Basin

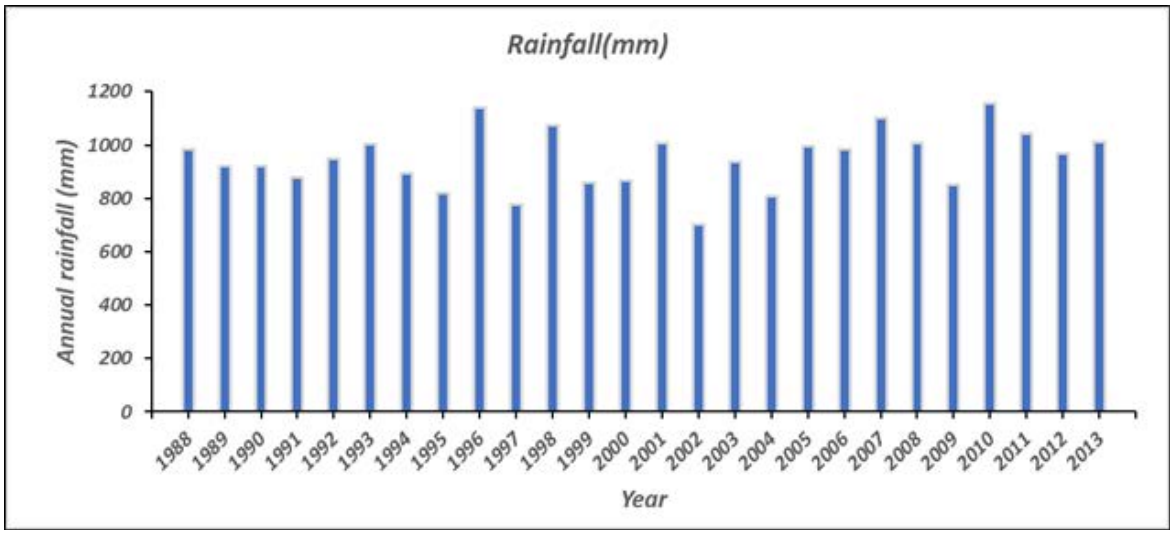

Figure 11: The Simulated Annual Rainfall in the Upper Awash Sub-Basin

For efficient water resource management and sustainable development, it's important to comprehend the ratio range of the water budget's constituent parts, as shown in Figure 12.

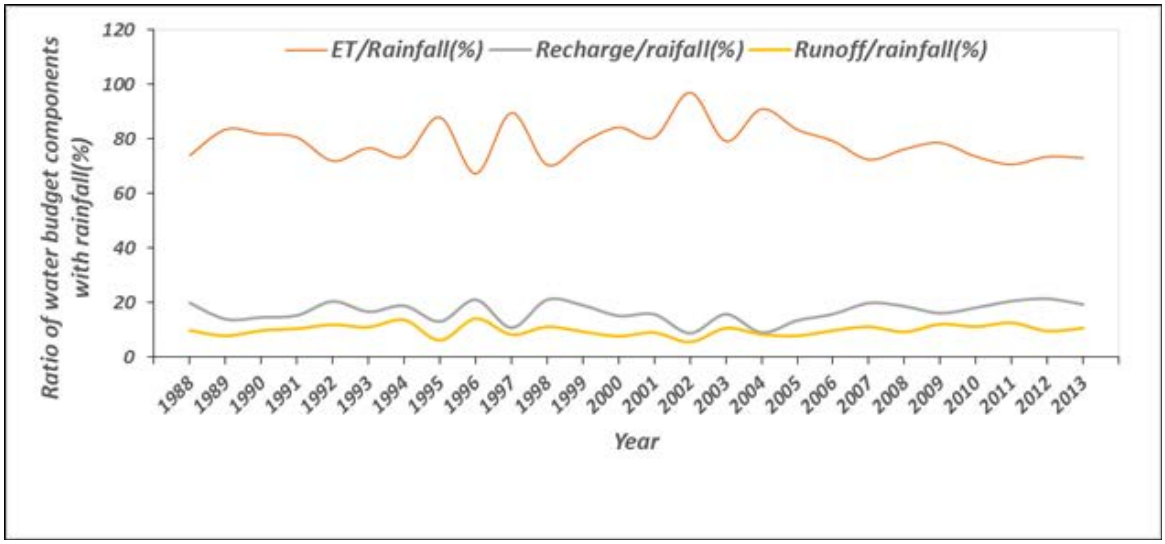

Figure 12: The Ratio of Rainfall to Water Budget Components in the Upper Awash Sub-Basin

Surface Runoff: Figure 13 illustrates the annual surface runoff within the study area. Estimated annual surface runoff in the sub-basin ranges from 0 mm to 240.5 mm, with a mean value of 93.4 mm/year and a standard deviation of 30.1 mm, according to the data analysis. These numbers reveal light on the surface runoff's variability and the sub basin's capacity for managing its water resources. The mean annual spatial pattern of the surface runoff in the sub-basin is shown in Figure 14. The graph demonstrates that the Hombele area, owns, and cities noticed the most considerable surface runoff (149.7-240.5 mm).

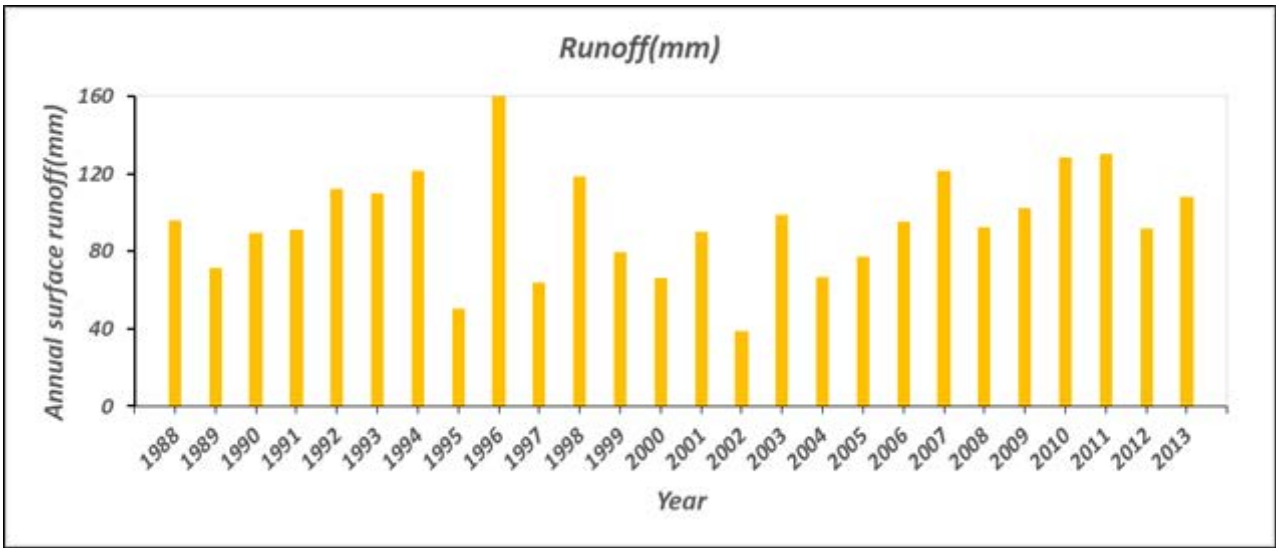

Figure 13: The Simulated Annual Surface Runoff in the Upper Awash Sub-Basin

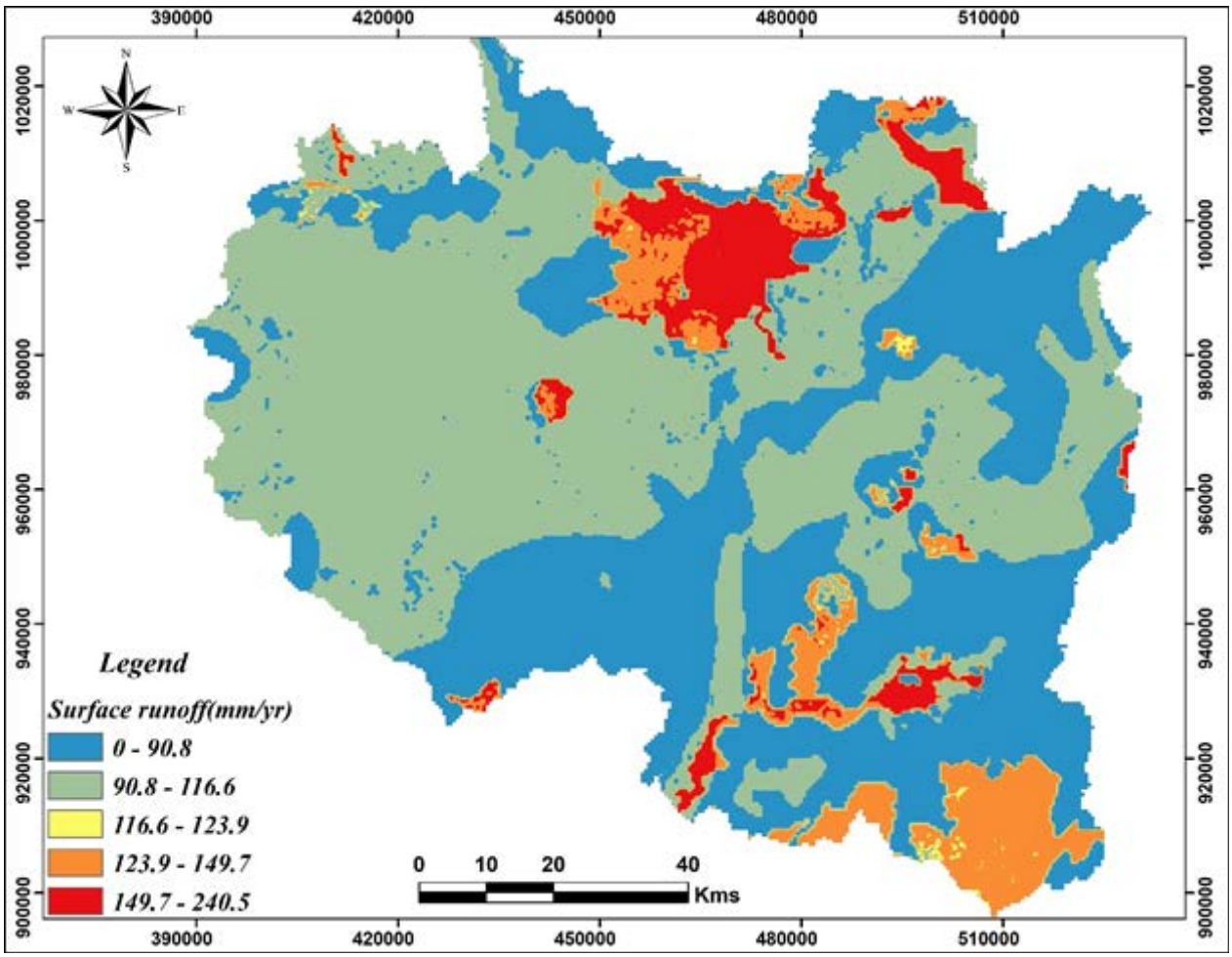

Figure 14: The Mean Annual Spatial Distribution of Surface Runoff

Citation: Muauz, A., Berehanu, B., Bedru, H. (2024). Spatial Analysis of Water Budget Components in the Upper Awash River Sub-basin, Ethiopia Using SWAT Model. Journal of Earth & Environmental Waste Management. 2(3), 1-23.

Evapotranspiration: The annual evapotranspiration in the upper Awash sub-basin ranges from 22.6 mm to 2237.8 mm, demonstrating significant variation. With a standard deviation of 200 mm, the average annual evapotranspiration in the basin is 682.5 mm. These figures highlight the critical role of evapotranspiration in the region's water budget, accounting for 71.8% of the annual rainfall. This indicates that a substantial portion of rainfall is lost to the atmosphere through evaporation and transpiration, impacting the management of water resources and the supply of water for both human and agricultural use. Figure 15 provides a visual representation of the annual evapotranspiration occurring within the study area. The spatial distribution of mean annual evapotranspiration reveals that open water bodies, such as Koka, Abasamuel, and lakes around Debrezeit, have high evapotranspiration rates, ranging from 1171.1 to 2237.8 mm, as shown in Figure 16.

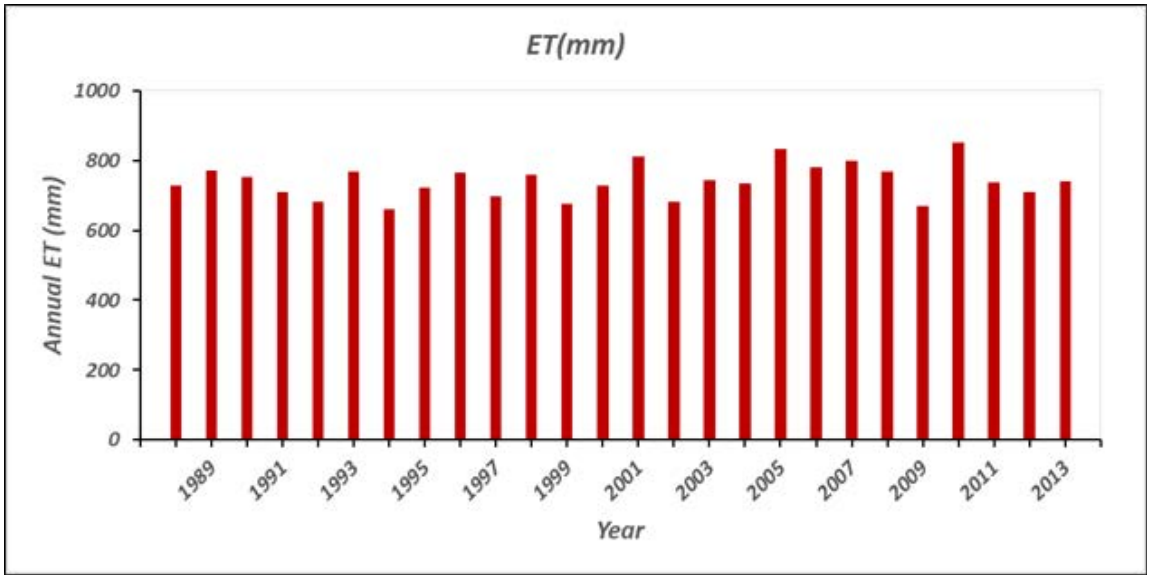

Figure 15: The Simulated Annual Evapotranspiration in the Upper Awash Sub-Basin

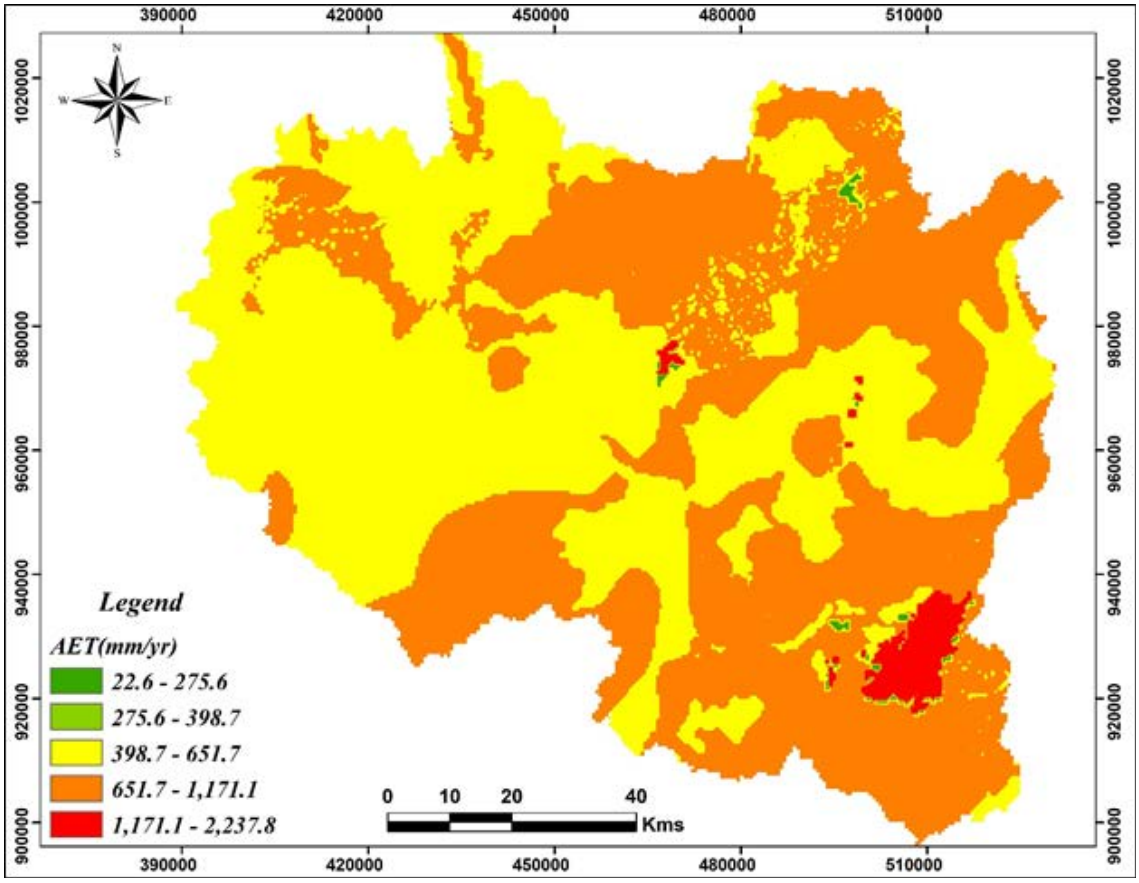

Figure 16: The Mean Annual Spatial Distribution of Evapotranspiration

Groundwater recharge: The bar chart depicted in Figure 17 represents the annual groundwater recharge within the study area. The annual groundwater recharge in the upper Awash River basin exhibits significant spatial variation, with values ranging between 0 and 904.3 mm, as depicted in Figure 18. The recharge estimation indicates that the total aquifer recharge for the entire basin, calculated using a long-term (28 years) mean annual recharge, equals 181.1 mm/year. This calculation comes with a standard deviation of 64.9 mm, representing 19.1% of the average annual rainfall. These figures highlight the variability in the area's groundwater recharge and underscore the potential for long-term groundwater management.

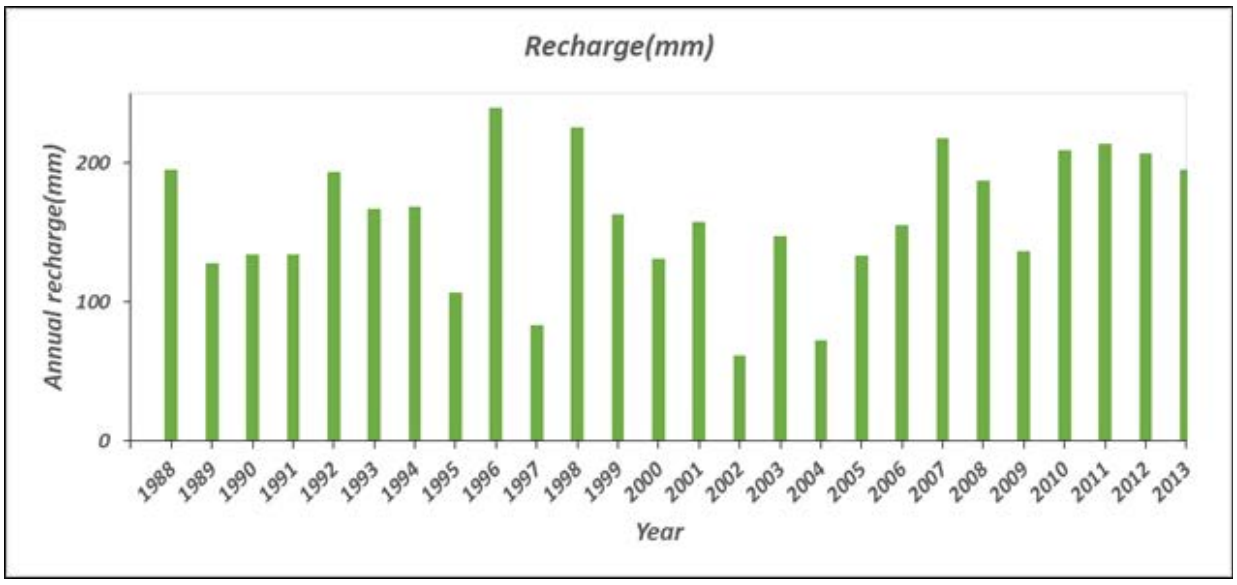

Figure 17: The Simulated Annual Groundwater Recharge in the Upper Awash Sub-Basin

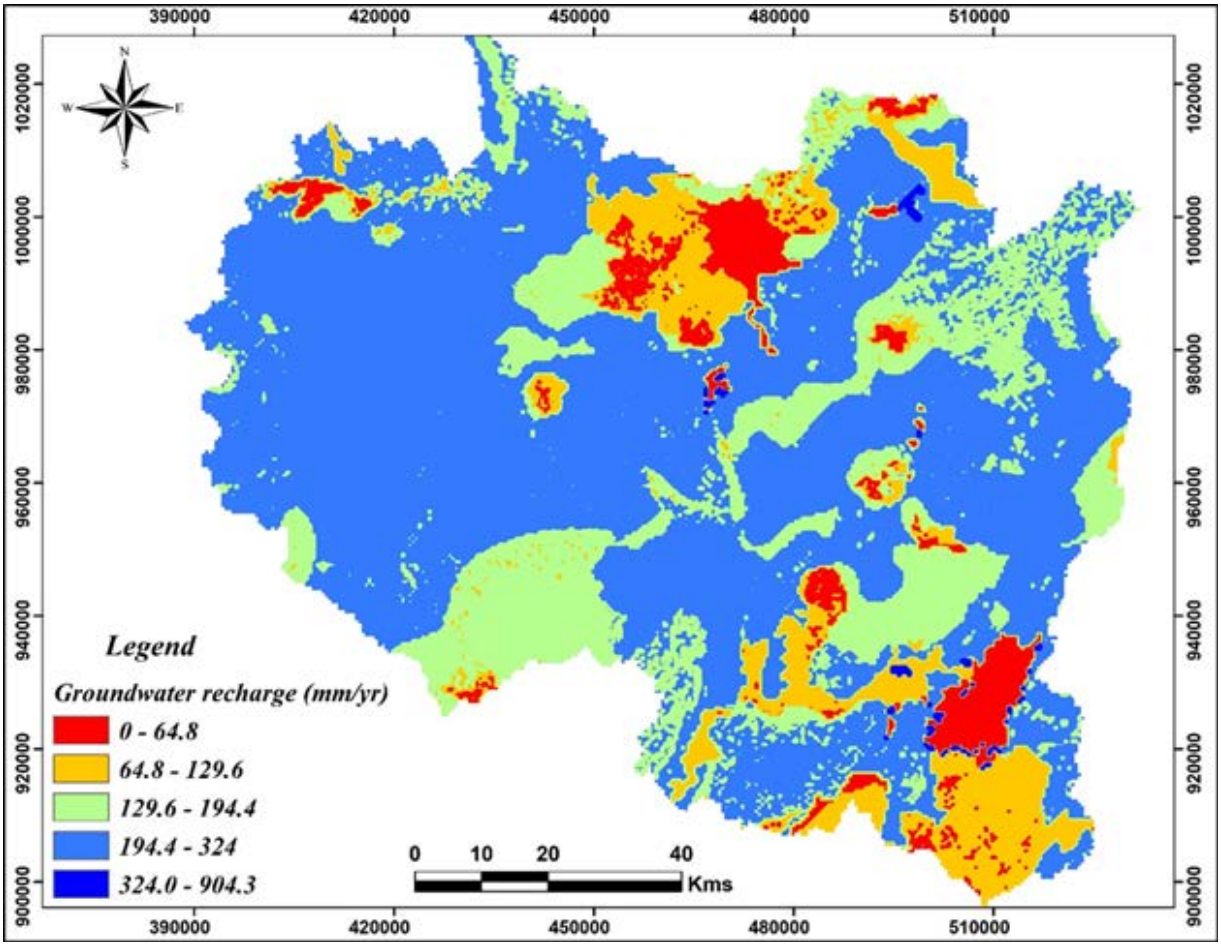

Figure 18: The Mean Annual Spatial Distribution of Groundwater Recharge

Citation: Muauz, A., Berehanu, B., Bedru, H. (2024). Spatial Analysis of Water Budget Components in the Upper Awash River Sub-basin, Ethiopia Using SWAT Model. Journal of Earth & Environmental Waste Management. 2(3), 1-23.

The study finds that agricultural land, designated as AGRL, exhibits the highest mean annual groundwater recharge value. This conclusion underscores the pivotal role of agricultural regions in sustaining water resources, as they significantly contribute to groundwater recharge. In contrast, urban (URBN) land use types are associated with the highest surface runoff values, indicating that urban areas contribute more to runoff compared to other land use types. Furthermore, land use/cover types encompassing aquatic bodies display the highest evapotranspiration values, suggesting these areas experience elevated rates of water loss through evaporation and transpiration. Conversely, water bodies land use/cover types exhibit the lowest mean annual groundwater recharge and surface runoff values, implying these areas make limited contributions to groundwater recharge and runoff. In contrast, urban (URBN) land use/cover types demonstrate the lowest evapotranspiration value, indicating that urban areas experience lower rates of water loss through evaporation and transpiration compared to other land use types. Figure 19 visually represents these disparities in mean annual groundwater recharge, surface runoff, and evapotranspiration values across different land use types.

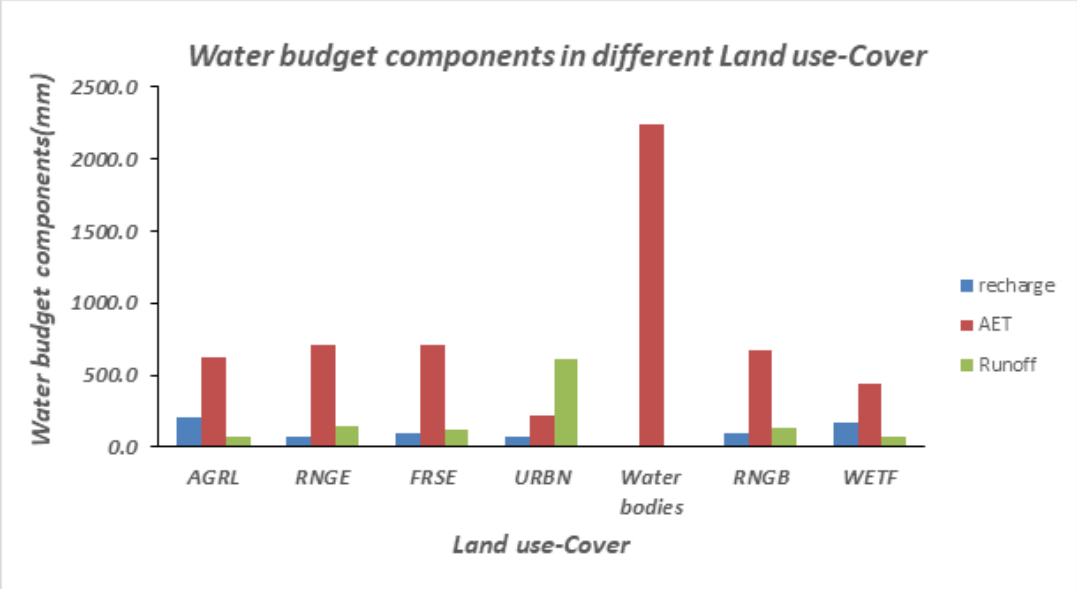

Figure 19: Actual Evapotranspiration, Recharge, and Surface Runoff Components in Different Land-Cover Use Units

4. Conclusions

The SWAT model was utilized to estimate the spatial distribution of groundwater recharge, surface runoff, and evapotranspiration. It also determined the long-term mean annual values for these parameters in the upper Awash sub-basin. The model generally produced good results, offering the advantage of providing separate values for each sub-basin's groundwater recharge, surface runoff, and evapotranspiration.

In the calibration phase, Hombele demonstrated p-factor and r-factor ratios of 0.801 and 0.97, respectively. This indicates that the model captured approximately 80.1% and 97% of the observed values for peak flows and flow volume. On the other hand, Melkakuntro presented slightly lower but still acceptable ratios of 0.808 and 0.98.

The calibration results for Hombele showed R2, NSE, and PBIAS values of 0.82, 0.82, and -2.3, respectively. These figures signify a strong fit between the simulated and observed data, with a high level of agreement between the two, despite a slight underestimation in the simulated data. Melkakuntro's calibration results displayed R2, NSE, and PBIAS values of 0.79, 0.78, and -13.1, respectively. These suggest a reasonably good fit and explain about 79% of the variability in the observed data. However, the PBIAS value indicates a more significant underestimation in the simulated data compared to the observed values than that of Hombele.

During validation, both Hombele and Melkakuntro exhibited satisfactory results. Hombele's R2, NSE, and PBIAS values were 0.71, 0.67, and 11.2, respectively, indicating a reasonable fit between the simulated and observed data. Melkakuntro showed R2, NSE, and PBIAS values of 0.7, 0.66, and 1.9, demonstrating a good agreement between the simulated and observed data.

The SWAT model findings revealed that the mean annual recharge in the upper Awash sub-basin is approximately 181.1 mm/year, accounting for 2.1 BCM/year and constituting about 19.1% of the total mean annual precipitation. The simulated mean annual surface runoff is 93.4 mm, or roughly 1.09 BCM, representing 9.4% of the mean annual precipitation. Evapotranspiration was estimated at 682.5 mm/year, making up 71.5% of the mean annual precipitation in the upper Awash sub-basin. The model's ability to represent processes spatially allows for an accurate depiction of spatial heterogeneity.

The water budget in this study may have been significantly influenced by hydro-meteorological data, flow data, climate change, and changes in land use. Therefore, future studies should consider the combined effects of several factors on the estimation of the water budget in the Upper Awash River sub-basin. Further research, data collection, and consideration of future changes are necessary to enhance the accuracy and applicability of the findings on water budget components in the Upper Awash River sub-basin.

Acknowledgments

The authors would like to express their gratitude to the Water and Energy Design and Supervision Works Sector (ECDSWC-WEDSWS) of the Ethiopian Construction Design and Supervision Corporation, The Ethiopian National Meteorological Agency (NMA) and the Ministry of Water and Energy (MoWE) for their valuable contribution to daily weather data and river flow data.

Reference

1. UN-Water, "Integrated Monitoring Guide for Sustainable Development Goal 6," Water Sanit., 2018.
2. Steduto, P., Faurès, J. M., Hoogeveen, J., Winpenny, J., & Burke, J. (2012). Coping with water scarcity: an action framework for agriculture and food security. Rome: Food and Agriculture Organization of the United Nations.
3. Oki, T., & Kanae, S. (2006). Global hydrological cycles and world water resources. science, 313(5790), 1068-1072.
4. Haddeland, I., Heinke, J., Biemans, H., Eisner, S., Flörke, M., Hanasaki, N., ... & Wisser, D. (2014). Global water resources affected by human interventions and climate change. Proceedings of the National Academy of Sciences, 111(9), 3251-3256.
5. Vörösmarty, C. J., McIntyre, P. B., Gessner, M. O., Dudgeon, D., Prusevich, A., et al. (2010). Global threats to human water security and river biodiversity. nature, 467(7315), 555-561.
6. Van Beek, L. P., Wada, Y., & Bierkens, M. F. (2011, December). Global Depletion of Groundwater Resources and Its Contribution to Sea-Level Rise. In AGU Fall Meeting Abstracts (Vol. 2011, pp. H14B-01).
7. Hanasaki, N., Fujimori, S., Yamamoto, T., Yoshikawa, S., Masaki, Y., Hijioka, Y., ... & Kanae, S. (2013). A global water scarcity assessment under Shared Socio-economic Pathways–Part 2: Water availability and scarcity. Hydrology and Earth System Sciences, 17(7), 2393-2413.
8. [8] et al Arnell, N. W., "Global-scale macroeconomic assessment of future drought impacts: a cross-sectoral analysis," Clim. Change, pp. 543–571, 2011.
9. Gleeson, T., Wada, Y., Bierkens, M. F., & Van Beek, L. P. (2012). Water balance of global aquifers revealed by groundwater footprint. Nature, 488(7410), 197-200.
10. Wada, Y., van Beek, L. P., & Bierkens, M. F. (2011). Modelling global water stress of the recent past: on the relative importance of trends in water demand and climate variability. Hydrology and Earth System Sciences, 15(12), 3785-3808.
11. [11] S. G. Dile, Y. T., Berndtsson, R., & Setegn, "Hydrological response to climate change for Gilgel Abbay catchment, Blue Nile basin, Ethiopia," Water Resour. Manag., pp. 1377–1395, 2013.
12. Mishra, A. K., & Singh, V. P. (2010). A review of drought concepts. Journal of hydrology, 391(1-2), 202-216.
13. [13] K. Guan, X., Zhu, X., & Hubacek, "Assessing urban water use in different climatic zones of China: A supply-chain and structural decomposition analysis," J. Clean. Prod., pp. 292–303, 2018.
14. S. Goswami, R. R., Shrestha, S., & Khanal, "Water budget analysis for river basins in Nepal," Environ. Process., pp. 1–16, 2019.
15. M. Singh, V. P., Knapp, H. V., & Demissie, "Hydrologic modeling in arid and semi-arid areas," Springer, 2015.
16. Wang, Y., Gu, X., Yang, G., Yao, J., & Liao, N. (2021). Impacts of climate change and human activities on water resources in the Ebinur Lake Basin, Northwest China. Journal of Arid Land, 13(6), 581-598.
17. [17] G. Zhang, Y., Wang, Y., & Huang, "Water resources allocation under multiple uncertainties: A case study in the Kaidu-Kongqi river basin, Northwest China," Water Resour. Manag., pp. 335–349, 2016.
18. Kebede, S., Travi, Y., Alemayehu, T., & Ayenew, T. (2005). Groundwater recharge, circulation and geochemical evolution in the source region of the Blue Nile River, Ethiopia. Applied Geochemistry, 20(9), 1658-1676.
19. [19] P. Gebrehiwot, S. G., Mohamed, Y. A., & van der Zaag, "Assessing the impacts of climate change on the hydrology of the Upper Blue Nile Basin using a distributed hydrological model," Hydrol. Earth Syst. Sci., pp. 563–585, 2018.
20. P. Gebrehiwot, S. G., Mohamed, Y. A., & van der Zaag, "A conceptual framework for hydrological drought in the Upper Blue Nile Basin, Ethiopia," Hydrol. Process., pp. 3680–3695, 2016.
21. R. Yihdego, Y., & Srinivasan, "Hydrological modeling of the Upper Blue Nile River Basin using SWAT model," Hydrol. Process., pp. 793–812, 2010.
22. Bewket, W., & Conway, D. (2007). A note on the temporal and spatial variability of rainfall in the drought-prone Amhara region of Ethiopia. International Journal of Climatology: A Journal of the Royal Meteorological Society, 27(11), 1467-1477.
23. [23] R. Getachew, H., Gebremichael, M., & Srinivasan, "Hydrologic response of the Upper Blue Nile Basin to climate change and implications for the Grand Ethiopian Renaissance Dam (GERD)," J. Hydrol. Reg. Stud., pp. 1–18, 2018.
24. D. Ayalew, D., & Molla, "Water balance estimation and assessment of hydrological drought in the Awash River Basin, Ethiopia," Hydrol. Res., pp. 1451–1468, 2019.
25. Allen, R. G., Pereira, L. S., Raes, D., & Smith, M. (1998). Crop evapotranspiration-Guidelines for computing crop water requirements-FAO Irrigation and drainage paper 56. Fao, Rome, 300(9), D05109.
26. Arnold, J. G., Moriasi, D. N., Gassman, P. W., Abbaspour, K. C., White, M. J., et al. (2012). SWAT: Model use, calibration, and validation. Transactions of the ASABE, 55(4), 1491-1508.

27. S. . Neitsch, J. . Arnold, J. . Kiniry, and J. . Williams, "Soil & Water Assessment Tool Theoretical Documentation Version 2009," Texas Water Resour. Inst., pp. 1–647, 2011, doi: 10.1016/j.scitotenv.2015.11.063.
28. Neitsch, S. L. (2005). Soil and water assessment tool. User's Manual Version 2005, 476.
29. Chow, V. T., Maidment, D. R., & Larry, W. (1988). Mays. Applied Hydrology. International edition, MacGraw-Hill, Inc, 149.
30. Arnold, J. G., & Allen, P. M. (1999). Automated methods for estimating baseflow and ground water recharge from streamflow records 1. JAWRA Journal of the American Water Resources Association, 35(2), 411-424.
31. Monteith, J. L. (1965). Evaporation and environment. pp. 205-234. In GE Fogg Symposium of the Society for Experimental Biology. The State and Movement of Water in Living Organisms, 19.
32. Priestley, C. H. B., & Taylor, R. J. (1972). On the assessment of surface heat flux and evaporation using large-scale parameters. Monthly weather review, 100(2), 81-92.
33. Hargreaves, G. H., & Samani, Z. A. (1985). Reference crop evapotranspiration from temperature. Applied engineering in agriculture, 1(2), 96-99.
34. Gassman, P. W., Reyes, M. R., Green, C. H., & Arnold, J. G. (2007). The soil and water assessment tool: historical development, applications, and future research directions. Transactions of the ASABE, 50(4), 1211-1250.
35. FAO, I., & ISRIC, I. (2012). Jrc: Harmonized world soil database (version 1.2). FAO, Rome, Italy and IIASA, Laxenburg, Austria.
36. van Griensven, A. V., Meixner, T., Grunwald, S., Bishop, T., Diluzio, M., et al. (2006). A global sensitivity analysis tool for the parameters of multi-variable catchment models. Journal of hydrology, 324(1-4), 10-23.
37. Abbaspour, K. C., Yang, J., Maximov, I., Siber, R., Bogner, K., Mieleitner, J., ... & Srinivasan, R. (2007). Modelling hydrology and water quality in the pre-alpine/alpine Thur watershed using SWAT. Journal of hydrology, 333(2-4), 413-430.
38. Abbaspour, K. C., Rouholahnejad, E., Vaghefi, S. R. I. N. I. V. A. S. A. N. B., Srinivasan, R., Yang, H., et al. (2015). A continental-scale hydrology and water quality model for Europe: Calibration and uncertainty of a high-resolution large-scale SWAT model. Journal of hydrology, 524, 733-752.
39. Santhi, C., Arnold, J. G., Williams, J. R., Dugas, W. A., Srinivasan, R., & Hauck, L. M. (2001). Validation of the swat model on a large rwer basin with point and nonpoint sources 1. JAWRA Journal of the American Water Resources Association, 37(5), 1169-1188.
40. Nash, J. E., & Sutcliffe, J. V. (1970). River flow forecasting through conceptual models part I—A discussion of principles. Journal of hydrology, 10(3), 282-290.
41. Gupta, H. V., Sorooshian, S., & Yapo, P. O. (1999). Status of automatic calibration for hydrologic models: Comparison with multilevel expert calibration. Journal of hydrologic engineering, 4(2), 135-143.
42. [42] V. Mockus and E. Engineer, "Section 4: Hydrology In National Engineering Handbook. SCS," 1992.
43. Allen, R. G., Pereira, L. S., Raes, D., & Smith, M. (1998). Crop evapotranspiration-Guidelines for computing crop water requirements-FAO Irrigation and drainage paper 56. Fao, Rome, 300(9), D05109.
44. Venetis, C. (1969). A study on the recession of unconfined acquifers. International Association of Scientific Hydrology. Bulletin, 14(4), 119-125.